國立臺灣大學電機資訊學院電信工程研究所
碩士論文
Graduate Institute of Communication Engineering
College of Electrical Engineering and Computer Science
National Taiwan University
Master Thesis

廣義分頻多工下的領導式通道估測

Pilot-aided Channel Estimation Methods for Generalized Frequency Division Multiplexing Systems

賈才
Cai Jia

指導教授：蘇柏青 博士
Advisor: Borching Su, Ph.D.

中華民國 108 年 1 月
January, 2019

doi:10.6342/NTU201902242

誌謝

這篇論文的完成，需要感謝很多人。俗話說，人生的學習是一輩子，即使在過程中會懷疑自己做的事情是否具有意義，倒頭來便會發現，有些事當下雖看不到意義何在，此後終將成為你成長的墊腳石，人生其實不虛度。完成此篇論文最大的感謝，就是我的指導教授蘇柏青。還記得初次認識他，我就認為我們想法很接近。面對問題許多人習慣按照書本上的方式解決，只求一個答案即可，即便自己沒有驗證過。但我認為既然已投資時間在一件事情上，就必須從頭到尾了解，用自己的思維去處理事情。在這一點上，教授和我有一樣的思維模式，我深深受蘇教授影響，他對於事情總保持獨立思考，寧願相信自己看到的，也不一昧相信權威的說法。其次，我很感謝戴敬倫與我的合作，這篇論文前期向他學習很多，也在他身上明白了只要有能力，即使你的頭銜還不夠閃亮，抑或遇到一些挫折，它們都無法抹滅你存在的價值。最後也感謝我實驗室裡遇到的同學們，與他們討論問題的過程中，我深刻體會每個人有著不同的學習歷程，因此影響其理解事物和表達的方法。我們在與他人溝通時，須盡量尊重每個人描述和理解事情的邏輯思維，即便那可能不符合自己的直覺，但有可能，是出自於經典書籍或所謂行業習慣說法，所謂存在即合理，慣用的東西必定有其形而上存在的道理在。我在研究所學到最重要的事，表達一件事情的重要性，不亞於事情本身，我會一輩子銘記在心。

doi:10.6342/NTU201902242

摘要

廣義分頻多工是次世代無線通訊系統頗具前途的波型候選人之一。然而，如何實踐廣義分頻多工的通道估測始終是一大挑戰，因其系統本身載波間通常為非正交而存在干擾。本論文首先提出一個基於預編碼器的領航符號插入架構，適用於廣泛的調變矩陣，包括了廣義分頻多工矩陣，並且針對預編碼器推導出了在接收端對應之最小均方誤差估計器。基於此架構我們進一步提出了一個可在接收端消除估測干擾之預編碼器，其透過了讓傳送訊號在頻域上的若干頻率點形成固定領航符號，進而消除若干頻率點上因資料符號之隨機性而產生的變動。模擬結果顯示我們提出的預編碼器相較於傳統的領航符號散佈方法，降低了通道估測的均方誤差與訊雜較高時的符號錯誤率。

關鍵字： 廣義分頻多工, 領航符號插入, 最小均方誤差估計器, 符號錯誤率

doi:10.6342/NTU201902242

Abstract

Generalized frequency division multiplexing (GFDM) is a promising candidate waveform for next-generation wireless communication systems. However, channel estimation is still challenging for GFDM due to its inherent interference. In this paper, we formulate a pilot-insertion framework based on a precoder design for block-based systems including GFDM and derive its linear minimum mean square error (LMMSE) channel estimator. We propose a solution for the precoder to achieve interference precancellation by generating the pilots at several tramsmit frequency bins and eliminating the randomness at such frequency bins due to data symbols. Numerical results demonstrate that the proposed method reduces the channel estimation mean square error and high signal-to-noise ratio (SNR) symbol error rate (SER), compared to conventional pilots scattering methods.

Keywords: Generalized frequency division multiplexing (GFDM), pilot-insertion, linear minimum mean square error (LMMSE) channel estimation, symbol error rate (SER)

doi:10.6342/NTU201902242

Contents

doi:10.6342/NTU201902242

doi:10.6342/NTU201902242

List of Figures

doi:10.6342/NTU201902242

Chapter 1

Introduction

Generalized frequency division multiplexing (GFDM), considered as a candidate waveform for next-generation wireless communication systems, features several advantages such as low out-of-band (OOB) emissions and relaxed requirements of time and frequency synchronizations [1]. Particularly, it has been shown in [2] that the GFDM systems have the potential to outperform OFDM systems by exploiting the frequency diversity. GFDM was often considered to be a non-orthogonal system with noise enhancement effect and MSE performance degradation compared to OFDM. However, [3] shows that based on the prototype filter design and the matrix characterization for GFDM, the mean square error of equalisation could be minimized and low-complexity transceiver could be implemented.

However, due to the inherent inter-subsymbol interference (ISI) and potential inter-subcarrier interference (ICI) accompanied with specific prototype filters, the received reference signal (i.e. pilots) is influenced by data symbols. Such impact of the data on pilot symbols degrades the channel estimation performance in comparison to orthogonal frequency division multiplexing (OFDM) which takes advantage of clear pilot observation. Therefore, the OFDM based channel estimations can not be directly adopted to GFDM.

Several methods like matched filter (MF) in [4, 5], orthogonal match pursuit (OMP) in [6], and the parallel interference cancellation(PIC) in [7] are adopted to further improve the channel estimation performance. However, the PIC method could get an additional complexity of cubic growth in receiver, MF approach is based on the assumption of nearly flat, slow fading channels, and the iterative OMP method cause a severe latency to the

doi:10.6342/NTU201902242

system, which are against the requirements of next-generation wireless communication systems.

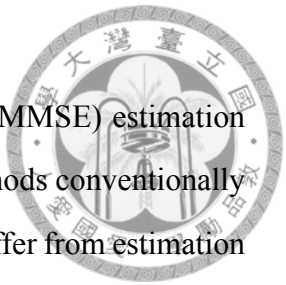

The least square (LS) and linear minimum mean square error (LMMSE) estimation in GFDM receiver have been adopted in [8–10]. However, these methods conventionally scatter the pilots in data block without any processing, which could suffer from estimation performance degradation due to the inherent interference of data symbols.

In [11], a technique called interference-free pilots insertion (IFPI) modify the waveform and structure of GFDM for orthogonal pilot insertion, subsequently achieving an interference-free channel estimation performance. However, such modification cause performance degradation including OOB emission and peak-to-average power ratio (PAPR).

In this paper, based on a block transmission [12] GFDM, we formulate a pilot-insertion framework including a general precoder which could be applied to both orthogonal and non-orthogonal waveforms. We derive its corresponding LMMSE channel estimator and propose a procedure which guarantees a solution for the precoder to achieve interference precancellation. By generating the pilots at several tramsmit frequency bins and eliminating the randomness at such frequency bins due to data symbols, the precoder leads to a significant improvement in LMMSE channel estimation accuracy compared to the conventional pilot-insertion [8–10]. With proper pilot arrangement, the computational complexity for pilot-insertion precoding could be very low, and there is no need for receiver to cancel the channel estimation interference. Our contribution in this paper:

- For GFDM and any other block-based communication systems, we formulate a general pilot-insertion framework with a flexible precoder design, and derive its corresponding LMMSE channel estimator.
- Based on the precoder, we formulate a condition which guarantees the interference cancellation for pilot-aided channel estimation.
- We propose a procedure which guarantees a solution for the precoder to cancel the interference.
- We show the proposed pilot-insertion prcoder for IFPI-GFDM [11] and explain its

doi:10.6342/NTU201902242

advantage on channel estimation.

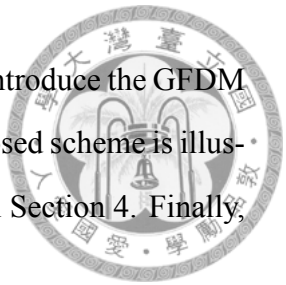

The remainder of this paper is organized as follows. In Section 2, we introduce the GFDM channel system model and channel reconstruction methods. The proposed scheme is illustrated in Section 3. Simulation results and discussion are presented in Section 4. Finally, a conclusion with the futurework is provided in Section 5.

Notations: Boldfaced capital and lowercase letters denote matrices and column vectors, respectively. We use $\mathrm{E}\{\cdot\}$ and $\langle . \rangle_D$ to denote the expectation operator and modulo D, respectively. Given a vector $\mathbf{u}$, we use $[\mathbf{u}]_n$ to denote the nth component of $\mathbf{u}$, $\|\mathbf{u}\|$ the ℓ_2-norm of $\mathbf{u}$, and $\mathrm{diag}(\mathbf{u})$ the diagonal matrix containing $\mathbf{u}$ on its diagonal. Given a matrix $\mathbf{A}$, we denote $[\mathbf{A}]_{m,n}$, $\mathrm{tr}(\mathbf{A})$, $\mathbf{A}^T$, $\mathbf{A}^*$, and $\mathbf{A}^H$ its (m, n)th entry (zero-based indexing), trace, transpose, complex conjugate, and Hermitian transpose, respectively. For two matrices $\mathbf{A}$, $\mathbf{B}$ of the same dimension , we denote $\circ$ as hadamard product. Given a diagnal matrix $\mathbf{D}$, We use $\mathrm{diag}^{-1}(\mathbf{D})$ to denote the vector containing the diagnal elements of $\mathbf{D}$. For any set $\mathcal{Q}$, we use $|\mathcal{Q}|$ to denote its cardinality. We adopt the MATLAB subscripts : and $a : b$ to denote all elements and the elements ordered from a to b, respectively, of the subscripted objects. Given index sets $\mathcal{I}, \mathcal{J} \subset \mathbb{Z}_{\geq 0} = \{0, 1, 2...\}$, we denote $[\mathbf{u}]_{\mathcal{I}}$ as the subvector of $\mathbf{u}$ containing the elements indexed by $\mathcal{I}$, $[\mathbf{A}]_{\mathcal{I},\mathcal{J}}$ as the submatrix of $\mathbf{A}$ containing the elements indexed by $\mathcal{I}, \mathcal{J}$, and $[\mathbf{A}]_{\mathcal{I},:}$, $[\mathbf{A}]_{:,\mathcal{J}}$ as the submatrix containing the rows, columns of $\mathbf{A}$ indexed by $\mathcal{I}$ and $\mathcal{J}$ respectively. We define $\mathbf{I}_q$ to be the $q \times q$ identity matrix, $\mathbf{0}_q$ the $q \times 1$ zero vector, $\mathbf{O}_{m,n}$ the $m \times n$ zero matrix. The $\mathbf{F}_q$,$\mathbf{W}_q$ are the q-point discrete Fourier transform (DFT) matrix and the normalized q-point DFT matrix with $[\mathbf{W}_q]_{m,n} = e^{-j2\pi mn/q}/\sqrt{q}, q \in \mathbb{N}$ and $[\mathbf{F}_q]_{m,n} = e^{-j2\pi mn/q} = \sqrt{q}\mathbf{W}_q$. For a $D \times 1$ vector $\mathbf{v}$, $d \times 1$ vector $\mathbf{p}$, and an indexes set $\mathcal{Q} \subset \{0, 1, 2, ..., D-1\}, |\mathcal{Q}| = d$, we use some columns of the identity matrix $\mathbf{I}_D$ as a $D \times d$ matrix $[\mathbf{I}_D]_{:,\mathcal{Q}}$ to generate $\mathbf{v} = [\mathbf{I}_D]_{:,\mathcal{Q}}\mathbf{p}$, where the elements in $\mathbf{p}$ are allocated in $[\mathbf{v}]_{\mathcal{Q}} = \mathbf{p}$ and other elements in $[\mathbf{v}]_{\{0,1,2,...,D-1\}-\mathcal{Q}} = \mathbf{0}_{D-|\mathcal{Q}|}$. For a $m \times n$ matrix $\mathbf{A}$, the collecting matrices $[\mathbf{I}_m]_{\mathcal{I},:}$ and $[\mathbf{I}_n]_{:,\mathcal{J}}$ satisfy $[\mathbf{I}_m]_{\mathcal{I},:}\mathbf{A}[\mathbf{I}_n]_{:,\mathcal{J}} = [\mathbf{A}]_{\mathcal{I},:}[\mathbf{I}_n]_{:,\mathcal{J}} = [\mathbf{I}_m]_{\mathcal{I},:}[\mathbf{A}]_{:,\mathcal{J}} = [\mathbf{A}]_{\mathcal{I},\mathcal{J}}$, where $[\mathbf{I}_m]_{\mathcal{I},:}$ and $[\mathbf{I}_n]_{:,\mathcal{J}}$ collect the rows and columns of $\mathbf{A}$ respectively. We define $\mathbf{L}_{D,L}$ to be the

doi:10.6342/NTU201902242

$(D+L)\times D$ cyclic prefix(CP) matrix, expressed as $\mathbf{L}_{D,L} = \begin{bmatrix} \mathbf{O}_{D+L,D-L} & \mathbf{I}_L \\ & \mathbf{I}_D \end{bmatrix}$ and the steering vector as $\mathbf{v}_D(e^{j\omega}) = \begin{bmatrix} 1\ e^{j\omega\cdot 1}\ e^{j\omega\cdot 2}...\ e^{j\omega\cdot(D-1)} \end{bmatrix}^T$. Given some matrices $\mathbf{A}, \mathbf{B}, \mathbf{C}...$, we define blkdiag$(\mathbf{A}, \mathbf{B}, \mathbf{C}...) = \begin{bmatrix} \mathbf{A} & \mathbf{O} & \mathbf{O} & \mathbf{O} \\ \mathbf{O} & \mathbf{B} & \mathbf{O} & \mathbf{O} \\ \mathbf{O} & \mathbf{O} & \mathbf{C} & \mathbf{O} \\ \mathbf{O} & \mathbf{O} & \mathbf{O} & ... \end{bmatrix}$.

doi:10.6342/NTU201902242

Chapter 2

System Model for GFDM Channel Estimation

2.1 GFDM System Model

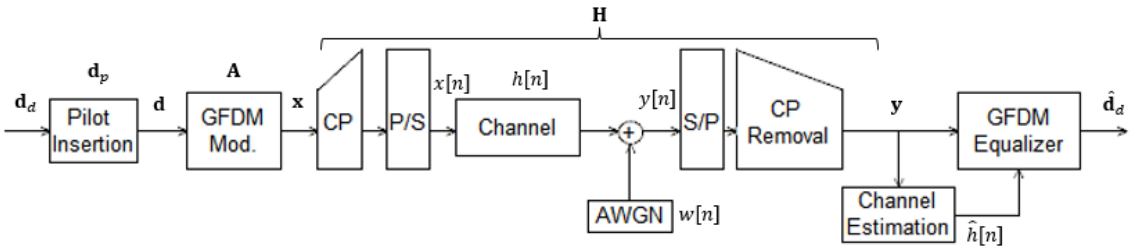

Figure 2.1: GFDM System Model with Channel Estimation

2.1.1 Transmitter

GFDM is a block-based communication scheme as shown in Fig. 2.1 [1,3]. Each GFDM block employs K subcarriers, with each transmitting M complex-valued subsymbols. So, a total of $D = KM$ symbols are transmitted in a block. Let $\mathbf{d}_l \in \mathbb{C}^D$ be the lth GFDM block, whose mth sybsymbol on the kth subcarrier is denoted as $[\mathbf{d}_l]_{k+mK}$, $m = 0, 1, ..., M-1, k = 0, 1, ..., K-1$.

Each symbol $[\mathbf{d}_l]_{k+mK}$ is pulse-shaped by a vector $\mathbf{g}_{k,m}$, whose nth entry is $[\mathbf{g}_{k,m}]_n = [\mathbf{g}_{0,0}]_{\langle n-mK \rangle_D} e^{j2\pi kn/K}$, $n = 0, 1, ..., D-1, m = 0, 1, ..., M-1, k = 0, 1, ..., K-1$, where

doi:10.6342/NTU201902242

$\mathbf{g}_{0,0} \in \mathbb{C}^D$ is called the *prototype filter* [1]. The GFDM transmitter matrix [1] could be collected by

$$\mathbf{A} = [\mathbf{g}_{0,0}...\mathbf{g}_{K-1,0}, \mathbf{g}_{0,1}...\mathbf{g}_{K-1,1}...\mathbf{g}_{K-1,M-1}], \tag{2.1}$$

and the transmit vector could be expressed as $\mathbf{x}_l = \mathbf{A}\mathbf{d}_l$, whose nth entry, for $n = 0, 1, ..., D-1$, is

$$[\mathbf{x}_l]_n = \sum_{k=0}^{K-1}\sum_{m=0}^{M-1}[\mathbf{d}_l]_{k+mK}[\mathbf{g}]_{\langle n-mK\rangle_D}e^{j2\pi kn/K}. \tag{2.2}$$

Subsequently, the vector $\mathbf{x}_l$ is passed through a parallel-to-serial (P/S) conversion, and a cyclic prefix (CP) of length L is further added. Denote the set of subcarrier indexes and set of subsymbol indexes that are actually employed as $\mathcal{K} \subseteq \{0, 1, ..., K-1\}$ and $\mathcal{M} \subseteq \{0, 1, ..., M-1\}$, respectively. The digital baseband transmit signal of GFDM can be expressed as [3]

$$x[n] = \sum_{l=-\infty}^{\infty}\sum_{k\in\mathcal{K}}\sum_{m\in\mathcal{M}}[\mathbf{d}_l]_{k+mK}g_m[n-lD']e^{j2\pi k(n-lD')/K}, \tag{2.3}$$

where $D' = D + L$ and

$$g_m[n] = \begin{cases} [\mathbf{g}]_{\langle n-mK-L\rangle_D}, & n = 0, 1, ..., D'-1 \\ 0, & \text{otherwise} \end{cases}. \tag{2.4}$$

For notational brevity, we omit the subscript l as in $\mathbf{x}_l$ and $\mathbf{d}_l$ hereafter.

2.1.2 Receiver

As shown in Fig. 2.1, the received signal after transmission through a wireless channel can be modeled as a linear time-invariant (LTI) system $y[n] = h[n] * x[n] + w[n]$, where $h[n]$ is the channel impulse response, and $w[n]$ is the complex additive white Gaussian noise (AWGN) with variance N_0. We denote $\mathbf{w} = [w[0]w[1]...w[D-1]]^T$ and $\mathbf{h} = [h[0]h[1]...h[N-1]]^T$, where $N-1$ is the channel order, as the vector forms of complex AWGN and channel impulse response, respectively. Note that $\mathbf{h} = \sqrt{\text{diag}(\mathbf{p})}\mathbf{q} \in \mathbb{C}^N$,

doi:10.6342/NTU201902242

where $\mathbf{p} \in \mathbb{C}^N$ is the power delay profile (PDP) and $\mathbf{q} \in \mathbb{C}^N$ is a vector of independently and identically distributed (i.i.d.) standard normal random variables, with the assumption that the channel order $N-1$ does not exceed the CP length L. After CP removal and serial-to-parallel (S/P) conversion, the received samples are collected as [7]

$$\begin{aligned}\mathbf{y} &= \mathbf{H}\mathbf{x} + \mathbf{w} = \mathbf{H}\mathbf{A}\mathbf{d} + \mathbf{w} \\ &= \mathbf{W}_D^H \text{diag}(\mathbf{F}_D \mathbf{h}_N)\mathbf{W}_D \mathbf{A}\mathbf{d} + \mathbf{w} \\ &= \mathbf{W}_D^H \text{diag}(\mathbf{W}_D \mathbf{A}\mathbf{d})\mathbf{F}_D \mathbf{h}_N + \mathbf{w},\end{aligned} \tag{2.5}$$

where $\mathbf{H} \in \mathbb{C}^{D\times D}$ is the circulant matrix whose first column is the channel impulse response $\mathbf{h}_N = [\mathbf{I}_D]_{:,\mathcal{N}}\mathbf{h} = [\mathbf{h}^T \quad \mathbf{0}_{D-N}^T]^T, \mathcal{N} = 0, 1, ..., N-1$.

2.2 OFDM Channel Estimation

The model in (2.5) could be adapted to OFDM system by substituting the IDFT matrix $\mathbf{W}_D^H$ for the modulation matrix $\mathbf{A}$. The received OFDM vector could be expressed as

$$\mathbf{y} = \mathbf{W}_D^H \text{diag}(\mathbf{d})\mathbf{F}_D \mathbf{h}_N + \mathbf{w}, \tag{2.6}$$

and

$$\mathbf{W}_D \mathbf{y} = \text{diag}(\mathbf{d})\mathbf{F}_D \mathbf{h}_N + \mathbf{W}_D \mathbf{w}, \tag{2.7}$$

in frequency domain. In OFDM receiver, the received vector $\mathbf{y}$ would be converted to frequency domain by $\mathbf{W}_D$ and each element in frequency domain received vector $[\mathbf{x}_f]_n = [\mathbf{W}_D\mathbf{y}]_n = [\mathbf{d}]_n[\mathbf{F}_D\mathbf{h}_N]_n + [\mathbf{W}_D\mathbf{w}]_n$ experiences a flat-fading channel as shown in Fig. 2.2. In order to obtain the channel state information (CSI), the several spaces indexed by $\mathcal{J}$ in the OFDM block $\mathbf{d}$ are employed to a reference vector $\mathbf{d}_r$ denoted as $[\mathbf{d}]_{\mathcal{J}} = \mathbf{d}_r$ for pilot-insertion, and the rest of spaces in $\mathbf{d}$ are reserved for the data vector $\mathbf{d}_s$, denoted as $[\mathbf{d}]_{\mathcal{I}} = \mathbf{d}_s$. By observing the received vector in frequency domain, the several spaces

doi:10.6342/NTU201902242

indexed by $\mathcal{J}$ could be collected as

$$\begin{aligned}[\mathbf{W}_D\mathbf{y}]_{\mathcal{J}} &= \text{diag}([\mathbf{d}]_{\mathcal{J}})[\mathbf{F}_D\mathbf{h}_N]_{\mathcal{J}} + [\mathbf{W}_D\mathbf{w}]_{\mathcal{J}} \\ &= \text{diag}(\mathbf{d}_r)[\mathbf{I}_D]_{\mathcal{J},:}\mathbf{F}_D[\mathbf{I}_D]_{:,\mathcal{N}}\mathbf{h} + [\mathbf{W}_D\mathbf{w}]_{\mathcal{J}} \\ &= \text{diag}(\mathbf{d}_r)[\mathbf{F}_D]_{\mathcal{J},\mathcal{N}}\mathbf{h} + [\mathbf{W}_D\mathbf{w}]_{\mathcal{J}},\end{aligned} \tag{2.8}$$

Assuming the effect of noise is ignored, and the number of the pilot symbols $|\mathcal{J}| \geq$ the

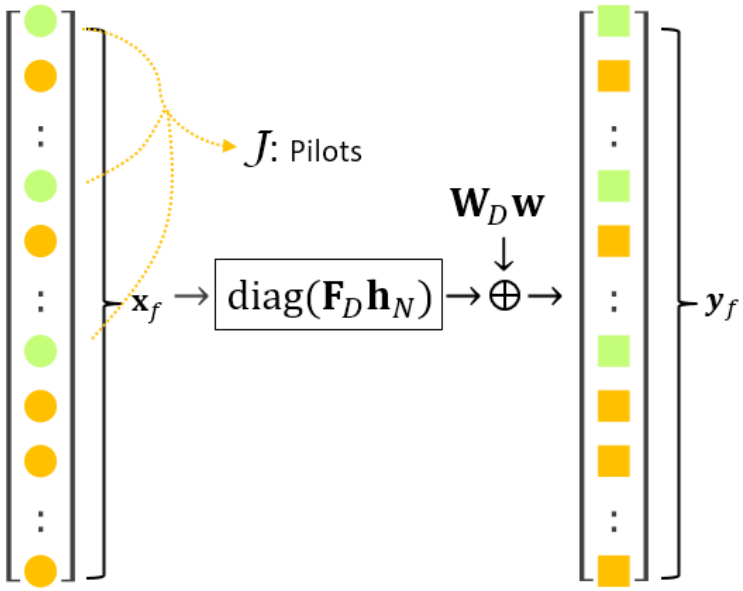

Figure 2.2: OFDM Channel Estimation with $\mathbf{x}_f = \mathbf{W}_D\mathbf{A}\mathbf{d}$ and $\mathbf{y}_f = \mathbf{W}_D\mathbf{y}$

channel length N, we could reconstruct the channel impulse vector with the knowledge of the reference vector $[\mathbf{d}]_{\mathcal{J}} = \mathbf{d}_r$, and

$$\hat{\mathbf{h}} = \text{pinv}([\mathbf{F}_D]_{\mathcal{J},\mathcal{N}})(\text{diag}(\mathbf{d}_r))^{-1}[\mathbf{W}_D\mathbf{y}]_{\mathcal{J}}, \tag{2.9}$$

where pinv$(\cdot)$ denotes the Moore-Penrose pseudoinverse.

doi:10.6342/NTU201902242

Chapter 3

Proposed Methods

In this section, the problem of channel estimation in GFDM is statemented. With the significant interference inherent in GFDM, the performance of channel estimation in existing literature [8–10] suffers from severe degradation, especially in high SNR, due to the lack of interference precancellation in pilot design.

3.1 The Problem of Channel Estimation in GFDM

In order to achieve the channel estimation at the receiver, the GFDM block $\mathbf{d}$ is generated from two subvectors, the pilot vector $\mathbf{d}_p \in \mathbb{C}^D$ and the data vector $\mathbf{d}_d \in \mathbb{C}^D$. The GFDM block $\mathbf{d}$ can be expressed as

$$\mathbf{d} = \mathbf{d}_p + \mathbf{d}_d. \tag{3.1}$$

In conventional pilot insertion framework, the pilot symbols and data symbols are allocated in data block $\mathbf{d}$ to be isolated from each other, which could be expressed as a linear transformation of $\mathbf{d}_r$ and $\mathbf{d}_s$, i.e.,

$$\mathbf{d} = [\mathbf{I}_D]_{:,\mathcal{J}}\mathbf{d}_r + [\mathbf{I}_D]_{:,\mathcal{I}}\mathbf{d}_s, \tag{3.2}$$

where the number of d data symbols in $\mathbf{d}_s \in \mathbb{C}^d$ are random source data variables with symbol energy E_s, and the number of p pilot symbols in $\mathbf{d}_r \in \mathbb{C}^p$ are deterministic reference elements. We choose the indexes set $\mathcal{I} \subset \{0, 1, ..., D-1\}$ and $[\mathbf{d}]_\mathcal{I}$ for data symbols with

doi:10.6342/NTU201902242

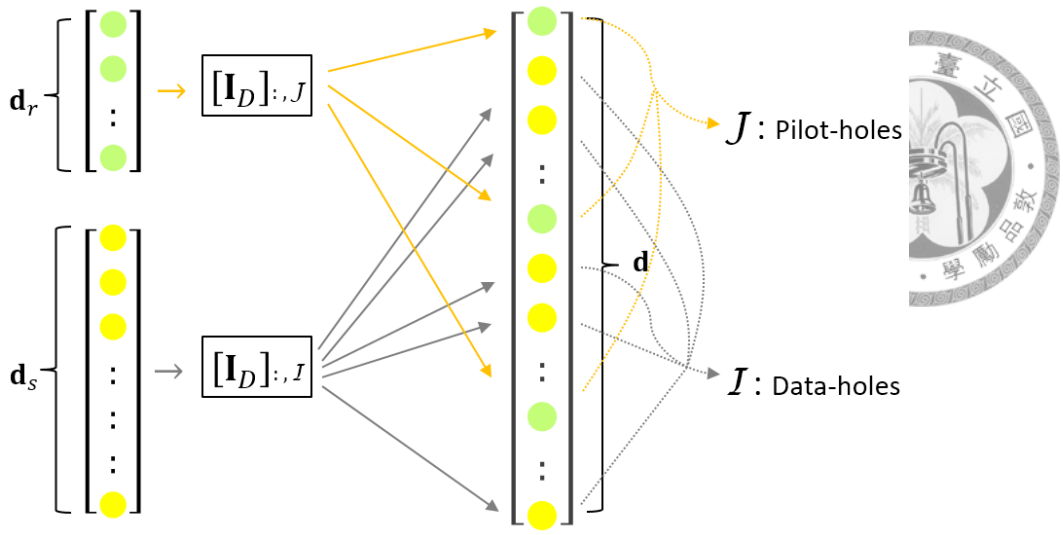

Figure 3.1: Conventional Pilot-insertion

$\mathcal{J} \subset \{0, 1, 2, ..., D-1\}$ and $[\mathbf{d}]_{\mathcal{J}}$ for pilot symbols, where $|\mathcal{I}| = d$, $|\mathcal{J}| = p$ and $\mathcal{I} \cap \mathcal{J} = \emptyset$. We call the pilot symbols in $[\mathbf{d}]_{\mathcal{J}}$ "pilot-holes" and data symbols in $[\mathbf{d}]_{\mathcal{I}}$ "data-holes". The matrices $[\mathbf{I}_D]_{:,\mathcal{J}} \in \mathbb{C}^{D\times p}$ and $[\mathbf{I}_D]_{:,\mathcal{I}} \in \mathbb{C}^{D\times d}$ are the corresponding allocating matrices of $\mathbf{d}_r$ and $\mathbf{d}_s$, which could determine the positions of pilot symbols and data symbols in data block $\mathbf{d}$ (illustrated in Fig. 3.1). Notice that $\mathbf{d}_d \circ \mathbf{d}_p = ([\mathbf{I}_D]_{:,\mathcal{J}}\mathbf{d}_r) \circ ([\mathbf{I}_D]_{:,\mathcal{I}}\mathbf{d}_s) = \mathbf{0}_D$, where elements in $[\mathbf{d}_d]_{\{0,1,2,...,D-1\}-\mathcal{I}}$ and $[\mathbf{d}_p]_{\{0,1,2,...,D-1\}-\mathcal{J}}$ are all zero.

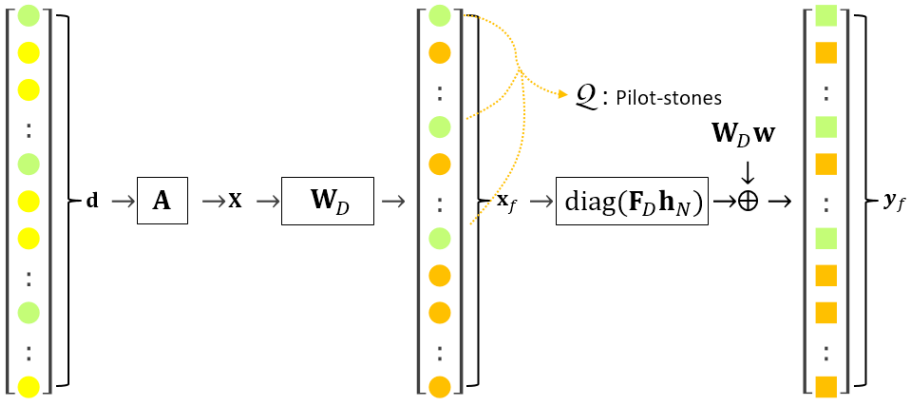

Figure 3.2: Pilot in Frequency Domain: The transmit symbols in frequency domain denoted by green circles(called "**pilot-stones**").

After modulation, we choose the number of p samples at $[\mathbf{x}_f]_{\mathcal{Q}}$ called **pilot-stones** (illustrated as green circles shown in Fig. 3.2), where $\mathcal{Q} \subset \{0, 1, ..., D-1\}, |\mathcal{Q}| = p$ is the pilot-stones indexes set. The relationship between $\mathbf{x}_f$ and $\mathbf{y}_f$, expressed as $\mathbf{y}_f = \text{diag}(\mathbf{F}_D\mathbf{h}_N)\mathbf{x}_f + \sqrt{D}\mathbf{W}_D\mathbf{w}$, benefits the frequency-domain channel estimation, where

doi:10.6342/NTU201902242

each element in $\mathbf{x}_f$ only corresponding to a flat-fading channel in $\text{diag}(\mathbf{F}_D\mathbf{h}_N)$. The pilot-stones in transmit frequency samples could be derived as

$$[\mathbf{x}_f]_{\mathcal{Q}} = [\mathbf{W}_D\mathbf{A}\mathbf{d}]_{\mathcal{Q}} = [\mathbf{W}_D\mathbf{A}([\mathbf{I}_D]_{:,\mathcal{J}}\mathbf{d}_r + [\mathbf{I}_D]_{:,\mathcal{I}}\mathbf{d}_s)]_{\mathcal{Q}}$$

$$= [\mathbf{W}_D\mathbf{A}[\mathbf{I}_D]_{:,\mathcal{J}}\mathbf{d}_r]_{\mathcal{Q}} + [\mathbf{W}_D\mathbf{A}[\mathbf{I}_D]_{:,\mathcal{I}}\mathbf{d}_s]_{\mathcal{Q}} = [\mathbf{W}_D\mathbf{A}]_{\mathcal{Q}}[\mathbf{I}_D]_{:,\mathcal{J}}\mathbf{d}_r + [\mathbf{W}_D\mathbf{A}]_{\mathcal{Q}}[\mathbf{I}_D]_{:,\mathcal{I}}\mathbf{d}_s =$$

$$[\mathbf{W}_D\mathbf{A}]_{\mathcal{Q},\mathcal{J}}\mathbf{d}_r + [\mathbf{W}_D\mathbf{A}]_{\mathcal{Q},\mathcal{I}}\mathbf{d}_s.$$

We expect to obtain a deterministic reference vector $\mathbf{d}_r$ in $[\mathbf{x}_f]_{\mathcal{Q}}$ (pilot-stones), so we formulate a condition called **pilot-stone condition** as

$$[\mathbf{x}_f]_{\mathcal{Q}} = [\mathbf{W}_D\mathbf{A}]_{\mathcal{Q},\mathcal{J}}\mathbf{d}_r + [\mathbf{W}_D\mathbf{A}]_{\mathcal{Q},\mathcal{I}}\mathbf{d}_s = \mathbf{d}_r, \tag{3.3}$$

which fixes the p frequency samples in $\mathbf{x}_f$ indexed by $\mathcal{Q}$. We could require the received frequency samples by $\mathcal{Q}$ as

$$[\mathbf{W}_D\mathbf{y}]_{\mathcal{Q}} = [\text{diag}(\mathbf{x}_f)\mathbf{F}_D\mathbf{h}_N + \mathbf{W}_D\mathbf{w}]_{\mathcal{Q}} = [\text{diag}(\mathbf{x}_f)]_{\mathcal{Q},:}\mathbf{F}_D\mathbf{h}_N + [\mathbf{W}_D\mathbf{w}]_{\mathcal{Q}}$$

$$= \text{diag}([\mathbf{x}_f]_{\mathcal{Q}})[\mathbf{F}_D]_{\mathcal{Q},\mathcal{N}}\mathbf{h} + [\mathbf{W}_D\mathbf{w}]_{\mathcal{Q}}, N \leq |\mathcal{Q}| = p. \tag{3.4}$$

The chosen pilot-stones $[\mathbf{x}_f]_{\mathcal{Q}}$ pass through a flat-fading channel $\text{diag}([\mathbf{F}_D]_{\mathcal{Q},\mathcal{N}}\mathbf{h})$ and become $[\mathbf{y}_f]_{\mathcal{Q}}$ (illustrated as green squares shown in Fig. 3.2) in which the corresponding elements in $\mathbf{d}_r$ get the channel information. With a deterministic $\mathbf{d}_r$ and the absence of noise in (3.4), the channel could be exactly reconstructed as

$$\hat{\mathbf{h}} = \text{pinv}([\mathbf{F}_D]_{\mathcal{Q},\mathcal{N}})\text{diag}(\mathbf{d}_r)^{-1}[\mathbf{W}_D\mathbf{y}]_{\mathcal{Q}}.$$

Notice that the channel can be exactly reconstructed only if the number of pilot symbols $|\mathcal{Q}| = p \geq N$ is satisfied, and as a special case $\mathcal{Q} = 0, M, 2M, ...(K-1)M$, $\mathcal{N} = 0, 1, ..., N-1$, where $|\mathcal{N}| < K$, we could find that $[\mathbf{F}_D]_{\mathcal{Q},\mathcal{N}} = [\mathbf{F}_D]_{\mathcal{Q},\{0,1,...,N-1\}} = [\mathbf{F}_K]_{:,\mathcal{N}}$ is a DFT submatrix and $\text{pinv}([\mathbf{F}_D]_{\mathcal{Q},\mathcal{N}})$ would become $([\mathbf{F}_D]_{\mathcal{Q},\mathcal{N}})^H$.

doi:10.6342/NTU201902242

The pilot-stone condition (3.3) guarantees the interference cancellation for pilot-aided channel estimation by fixing p pilot-stones in $[\mathbf{x}_f]_{\mathcal{Q}}$ and exactly reconstructing the channel with the knowledge of $[\text{diag}(\mathbf{x}_f)]_{\mathcal{Q},:} = \mathbf{d}_r$ and $[\mathbf{F}_D]_{\mathcal{Q},\mathcal{N}}$ in (3.4). To satisfy the pilot-stone condition (3.3), the conventional pilot-insertion depends on the choice of the modulation matrix $\mathbf{A}$, the pilot-stone indexes set $\mathcal{Q}$, pilot-hole indexes set $\mathcal{J}$ and the data-hole indexes set $\mathcal{I}$. For a classic OFDM case, the modulation matrix $\mathbf{A}$ is chosen as an identity IDFT matrix $\mathbf{W}_D^H$. Substituting $\mathbf{W}_D^H$ into the pilot-stone condition, the pilot-stones vector could be derived as

$$[\mathbf{x}_f]_{\mathcal{Q}} = [\mathbf{W}_D\mathbf{A}\mathbf{d}]_{\mathcal{Q}} = [\mathbf{d}]_{\mathcal{Q}} = [\mathbf{I}_D]_{\mathcal{Q},\mathcal{J}}\mathbf{d}_r + [\mathbf{I}_D]_{\mathcal{Q},\mathcal{I}}\mathbf{d}_s.$$

With the choice of $\mathcal{Q} = \mathcal{J}$, we could cancel the interference of data by $[\mathbf{I}_D]_{\mathcal{Q},\mathcal{I}}\mathbf{d}_s = [\mathbf{I}_D]_{\mathcal{J},\mathcal{I}}\mathbf{d}_s = \mathbf{0}_p$ and get the pilot-stones $[\mathbf{x}_f]_{\mathcal{Q}} = [\mathbf{I}_D]_{\mathcal{J},\mathcal{J}}\mathbf{d}_r + [\mathbf{I}_D]_{\mathcal{J},\mathcal{I}}\mathbf{d}_s = \mathbf{d}_r$. The OFDM transmit symbols in frequency domain $[\mathbf{x}_f] = \mathbf{W}_D\mathbf{A}\mathbf{d}$ is equal to the data block $\mathbf{d}$, hence the pilot-stones $[\mathbf{x}_f]_{\mathcal{Q}}$ would be equal to the reference vector $\mathbf{d}_r$ by choosing the indexes set $\mathcal{Q} = \mathcal{J}$, where $[\mathbf{d}]_{\mathcal{Q}} = [\mathbf{d}]_{\mathcal{J}} = \mathbf{d}_r$. However, the choice of $\mathcal{Q} = \mathcal{J}$ for other modulation matrices like GFDM could not guarantee $[\mathbf{W}_D\mathbf{A}]_{\mathcal{Q},\mathcal{I}}\mathbf{d}_s$ in (3.3) to be zero and the interference could not be canceled. Pilot-stone condition guarantees the interference cancellation for pilot-aided channel estimation. We reformulate a general pilot-insertion precoder for any modulation matrix $\mathbf{A}$ which could be further designed to satisfy the pilot-stone condition and its corresponding LMMSE channel estimator will be derived. Subsequently, we show a procedure which guarantees a solution for the precoder as our proposed method.

doi:10.6342/NTU201902242

3.2 Pilot-insertion Framework

3.2.1 Precoder Design

The data block $\mathbf{d}$ can be expressed as

$$\mathbf{d} = \mathbf{d}_p + \mathbf{d}_d. \tag{3.5}$$

We reformulate a general precoder by the linear transformation of $\mathbf{d}_r$ and $\mathbf{d}_s$, i.e.,

$$\mathbf{d} = \mathbf{S}\mathbf{d}_r + \mathbf{T}\mathbf{d}_s, \tag{3.6}$$

where $\mathbf{d}_r \in \mathbb{C}^p$ is the reference vector, $\mathbf{d}_s \in \mathbb{C}^d$ is the source data vector, and p, d denote the resource number of pilot and data. The matrices $\mathbf{S} \in \mathbb{C}^{D\times p}$ and $\mathbf{T} \in \mathbb{C}^{D\times d}$ are the corresponding linear coefficient matrices of $\mathbf{d}_r$ and $\mathbf{d}_s$, where $\mathbf{S}$ and $\mathbf{T}$ could be any precoding matrices. Assume that $\mathbf{d}_r$ and $\mathbf{d}_s$ are independent, and the symbols in $\mathbf{d}_s$ are zero-mean and i.i.d. with symbol energy E_s, we could get $\mathrm{E}\{\mathbf{d}\mathbf{d}^H\} = \mathbf{S}\,\mathrm{E}\{\mathbf{d}_r\mathbf{d}_r^H\}\mathbf{S}^H + E_S\mathbf{T}\mathbf{T}^H$. With different choices of the precoder $\mathbf{S}$ and $\mathbf{T}$, the $\mathbf{d}_p = \mathbf{S}\mathbf{d}_r$, $\mathbf{d}_d = \mathbf{T}\mathbf{d}_s$ in (3.6) are accordingly modified, and the data block $\mathbf{d} = \mathbf{d}_p + \mathbf{d}_d$ is generated by the linear combination of $\mathbf{d}_r$ and $\mathbf{d}_s$. As a special case of the conventional pilot-insertion methods [8–10], the matrices $\mathbf{S}$ and $\mathbf{T}$ are set to be $\mathbf{S} = [\mathbf{I}_D]_{:,\mathcal{J}}$ and $\mathbf{T} = [\mathbf{I}_D]_{:,\mathcal{I}}$. Based on a more flexible precoder design, more requirements could be achieved.

3.2.2 LMMSE Channel Estimation

In the following theorem, we derive the LMMSE channel estimator corresponding to the pilot-insertion precoder.

Theorem 1. *Given any modulation matrix* $\mathbf{A}$ *with the received samples* $\mathbf{y}$ *as defined in (2.5), the LMMSE estimated channel* $\hat{\mathbf{h}}_{LMMSE}$ *can be derived as*

$$\hat{\mathbf{h}}_{LMMSE} = \mathbf{G}_{LMMSE}\mathbf{y}, \tag{3.7}$$

doi:10.6342/NTU201902242

with

$$\mathbf{G}_{LMMSE} = \boldsymbol{\Sigma}_{hh}(\mathbf{X}_r[\mathbf{F}_D]_{:,N})^H \cdot [(\mathbf{X}_r[\mathbf{F}_D]_{:,N})\boldsymbol{\Sigma}_{hh}(\mathbf{X}_r[\mathbf{F}_D]_{:,N})^H + \boldsymbol{\Sigma}_{\Psi\Psi} + N_0\mathbf{I}_D]^{-1}\mathbf{W}_D, \tag{3.8}$$

where $\mathbf{X}_r = diag(\mathbf{W}_D\mathbf{A}\mathbf{S}\mathbf{d}_r)$, $\boldsymbol{\Sigma}_{hh} = \mathrm{E}\{\mathbf{h}\mathbf{h}^H\} = diag(\mathbf{p})$,
and $\boldsymbol{\Sigma}_{\Psi\Psi} = ([\mathbf{F}_D]_{:,N}\boldsymbol{\Sigma}_{hh}[\mathbf{F}_D]_{:,N}^H)(\mathbf{W}_D\mathbf{A}\mathbf{T}\mathbf{T}^H\mathbf{A}^H\mathbf{W}_D^H)$.

Proof. Proof of Theorem 1

Let the channel estimator be $\mathbf{G}$, and $\hat{\mathbf{h}} = \mathbf{G}\mathbf{y}$ is the estimated channel. Note that $\mathrm{diag}(\mathbf{W}_D\mathbf{A}\mathbf{d}) = \mathbf{X}_r + \mathbf{X}_s$. First, we derive the expected square error of channel estimation $\mathrm{E}\{\|\mathbf{h} - \mathbf{G}\mathbf{y}\|^2\}$ as

$$\begin{aligned}
&\mathrm{E}\{\mathrm{tr}((\mathbf{h} - \mathbf{G}\mathbf{y})(\mathbf{h} - \mathbf{G}\mathbf{y})^H)\} \\
&= \mathrm{tr}(\boldsymbol{\Sigma}_{hh} - \mathrm{E}\{\mathbf{h}\mathbf{y}^H\mathbf{G}^H\} - \mathrm{E}\{\mathbf{G}\mathbf{y}\mathbf{h}^H\} + \mathrm{E}\{\mathbf{G}\mathbf{y}\mathbf{y}^H\mathbf{G}^H\}) \\
&= \mathrm{tr}(\boldsymbol{\Sigma}_{hh}) - \mathrm{tr}(\boldsymbol{\Sigma}_{hh}(\mathbf{W}_D^H\mathbf{X}_r[\mathbf{F}_D]_{:,N})^H\mathbf{G}^H) \\
&- \mathrm{tr}(\mathbf{G}(\mathbf{W}_D^H\mathbf{X}_r[\mathbf{F}_D]_{:,N})\boldsymbol{\Sigma}_{hh}) + \mathrm{tr}(\mathbf{G}[\mathbf{W}_D^H(\mathbf{X}_r[\mathbf{F}_D]_{:,N})\boldsymbol{\Sigma}_{hh} \cdot \\
&(\mathbf{X}_r[\mathbf{F}_D]_{:,N})^H\mathbf{W}_D + \mathbf{W}_D^H\boldsymbol{\Sigma}_{\Psi\Psi}\mathbf{W}_D + N_0\mathbf{I}_D]\mathbf{G}^H).
\end{aligned} \tag{3.9}$$

The Wirtinger derivatives of $\mathrm{E}\{\|\mathbf{h} - \mathbf{G}\mathbf{y}\|^2\}$ with regard to $\mathbf{G}^*$ are obtained as [13]

$$\begin{aligned}
\frac{\partial\,\mathrm{E}\{\|\mathbf{h} - \mathbf{G}\mathbf{y}\|^2\}}{\partial\mathbf{G}^*} = &- \boldsymbol{\Sigma}_{hh}(\mathbf{X}_r[\mathbf{F}_D]_{:,N})^H\mathbf{W}_D + \mathbf{G}[\mathbf{W}_D^H(\mathbf{X}_r[\mathbf{F}_D]_{:,N})\boldsymbol{\Sigma}_{hh} \cdot \\
&(\mathbf{X}_r[\mathbf{F}_D]_{:,N})^H\mathbf{W}_D + \mathbf{W}_D^H\boldsymbol{\Sigma}_{\Psi\Psi}\mathbf{W}_D + N_0\mathbf{I}_D].
\end{aligned} \tag{3.10}$$

To solve for the optimal estimator, we require the derivatives to be zero and derive that

$$\begin{aligned}
\mathbf{G}_{\mathrm{LMMSE}} = &\boldsymbol{\Sigma}_{hh}(\mathbf{X}_r[\mathbf{F}_D]_{:,N})^H \cdot \\
&[(\mathbf{X}_r[\mathbf{F}_D]_{:,N})\boldsymbol{\Sigma}_{hh}(\mathbf{X}_r[\mathbf{F}_D]_{:,N})^H + \boldsymbol{\Sigma}_{\Psi\Psi} + N_0\mathbf{I}_D]^{-1}\mathbf{W}_D.
\end{aligned} \tag{3.11}$$

□

doi:10.6342/NTU201902242

For any modulation matrix $\mathbf{A}$ with the precoder $\mathbf{S}$,$\mathbf{T}$, a LMMSE channel estimation could be done by $\hat{\mathbf{h}}_{\text{LMMSE}} = \mathbf{G}_{\text{LMMSE}}\mathbf{y}$.

3.3 Interference-canceled Pilot Insertion Precoder

3.3.1 Pilot-stone Condition

The $\mathbf{S}$, $\mathbf{T}$ precoder provide the flexibility of pilot-insertion for any modulation matrix $\mathbf{A}$ to satisfy the pilot-stone condition which guarantees the interference reduction for pilot-aided channel estimation. The pilot-stone condition of the general pilot-insertion framework could be expressed as

$$[\mathbf{x}_f]_{\mathcal{Q}} = \mathbf{d}_r = [\mathbf{W}_D\mathbf{A}(\mathbf{S}\mathbf{d}_r + \mathbf{T}\mathbf{d}_s)]_{\mathcal{Q}}, \tag{3.12}$$

where the transmit frequency samples vector $[\mathbf{x}_f]_{\mathcal{Q}} = [\mathbf{W}_D\mathbf{A}\mathbf{d}]_{\mathcal{Q}} = [\mathbf{W}_D\mathbf{A}(\mathbf{S}\mathbf{d}_r + \mathbf{T}\mathbf{d}_s)]_{\mathcal{Q},:}$ is indexed by $\mathcal{Q} \subset \{0, 1, ..., D-1\}$,$|\mathcal{Q}| = p$. We choose $|\mathcal{Q}| = p$ samples in $\mathbf{x}_f$ to be a constant reference vector $\mathbf{d}_r$ and the pilot-stone condition (3.12) could be expressed as

$$\mathbf{d}_r = [\mathbf{W}_D\mathbf{A}\mathbf{S}]_{\mathcal{Q},:}\mathbf{d}_r + [\mathbf{W}_D\mathbf{A}\mathbf{T}]_{\mathcal{Q},:}\mathbf{d}_s. \tag{3.13}$$

and further derived as

$$\begin{aligned} [\mathbf{W}_D\mathbf{A}\mathbf{S}]_{\mathcal{Q},:} &= \mathbf{I}_p, \\ [\mathbf{W}_D\mathbf{A}\mathbf{T}]_{\mathcal{Q},:} &= \mathbf{O}_{p,d}. \end{aligned} \tag{3.14}$$

Given any modulation matrix $\mathbf{A}$, the precoder $\mathbf{S}$, $\mathbf{T}$ and the indexes set $\mathcal{Q}$ are designed to satisfy the pilot-stone condition.

3.3.2 Proposed Procedure for The Precoder Design

To find the precoder $\mathbf{S}, \mathbf{T}$ which satisfies (3.14), we propose a procedure which guarantees a solution for the precoder to satisfy the pilot-stone condition. Considering the pilot-insertion complexity and the non-interference of pilot and data, we reformulate the

doi:10.6342/NTU201902242

precoder **S**,**T** as

$$\begin{aligned}\mathbf{S} &= [\mathbf{I}_D]_{:,\mathcal{J}}\mathbf{C},\\ \mathbf{T} &= [\mathbf{I}_D]_{:,\mathcal{I}} - [\mathbf{I}_D]_{:,\mathcal{J}}\mathbf{D},\end{aligned} \tag{3.15}$$

where the precoder **S**, **T** for pilot-insertion are generated by two smaller matrices $\mathbf{C} \in \mathbb{C}^{p\times p}$ and $\mathbf{D} \in \mathbb{C}^{p\times d}$ with the allocating matrices $[\mathbf{I}_D]_{:,\mathcal{J}}$ and $[\mathbf{I}_D]_{:,\mathcal{I}}$. The data block **d** can be expressed by **C**, **D** as

$$\begin{aligned}\mathbf{d} &= [\mathbf{I}_D]_{:,\mathcal{J}}\mathbf{C}\mathbf{d}_r + ([\mathbf{I}_D]_{:,\mathcal{I}} - [\mathbf{I}_D]_{:,\mathcal{J}}\mathbf{D})\mathbf{d}_s\\ &= [\mathbf{I}_D]_{:,\mathcal{J}}(\mathbf{C}\mathbf{d}_r - \mathbf{D}\mathbf{d}_s) + [\mathbf{I}_D]_{:,\mathcal{I}}\mathbf{d}_s,\end{aligned} \tag{3.16}$$

where the indexes sets $\mathcal{I}, \mathcal{J} \subset \{0, 1, ..., D-1\}$ are designed to allocate the data symbols and pilot symbols in data block **d** (illustrated in Fig. 3.3). We set the condition $\mathcal{I} \cap \mathcal{J} = \emptyset$ to isolate the data symbols from pilot symbols in data block **d**, which implies $[\mathbf{d}]_{\mathcal{I}} = \mathbf{d}_s$ (illustrated as gray lines shown in Fig. 3.3). Notice that $|\mathcal{I}| = d$ is equal to the corresponding source data number, and $|\mathcal{J}| = p$ is equal to the number of the corresponding pilot symbols in the reference vector $\mathbf{d}_r$, where $d + p \leq D$. The elements in $[\mathbf{d}]_{\mathcal{I}}$ are directly generated by $\mathbf{d}_s$ and transferred to the locations only for data symbols indexed by $\mathcal{I}$. Notice that in Fig. 3.3 red lines passed through $-\mathbf{D}$ denote the extra processes for our proposed methods, and in the conventional pilot-insertion the matrix **D** is a zero matrix $\mathbf{O}_{p,d}$. To satisfy the pilot-stone condition, we substitute (3.15) into the equation (3.14), and get

$$\begin{aligned}\mathbf{C} &= ([\mathbf{W}_D\mathbf{A}]_{\mathcal{Q},\mathcal{J}})^{-1},\\ \mathbf{D} &= [\mathbf{W}_D\mathbf{A}]_{\mathcal{Q},\mathcal{J}})^{-1}[\mathbf{W}_D\mathbf{A}]_{\mathcal{Q},\mathcal{I}}.\end{aligned} \tag{3.17}$$

Notice that (3.17) exist if and only if the indexes set $\mathcal{Q}, \mathcal{J}$ mentioned above is chosen such that the matrix $[\mathbf{W}_D\mathbf{A}]_{\mathcal{Q},\mathcal{J}}$ is invertible. Finally, the proposed precoder **S** and **T** can be expressed as

$$\begin{aligned}\mathbf{S} &= [\mathbf{I}_D]_{:,\mathcal{J}}([\mathbf{W}_D\mathbf{A}]_{\mathcal{Q},\mathcal{J}})^{-1},\\ \mathbf{T} &= [\mathbf{I}_D]_{:,\mathcal{I}} - [\mathbf{I}_D]_{:,\mathcal{J}}([\mathbf{W}_D\mathbf{A}]_{\mathcal{Q},\mathcal{J}})^{-1}[\mathbf{W}_D\mathbf{A}]_{\mathcal{Q},\mathcal{I}}.\end{aligned} \tag{3.18}$$

The proposed procedure (3.15) carry out a solution for the precoder to satisfy the pilot-stone condition. The proposed precoder **S**,**T** in (3.18) could precancel inherent interfer-

doi:10.6342/NTU201902242

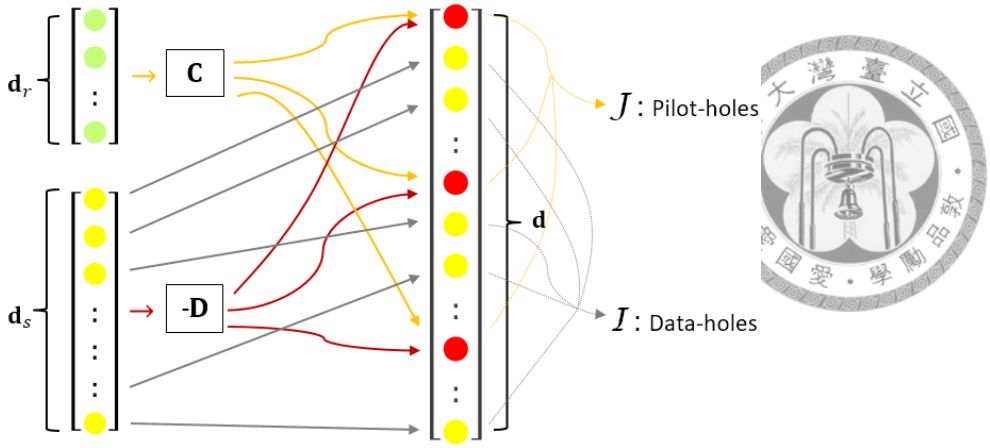

Figure 3.3: Pilot-insertion: Green solid circles denotes the deterministic elements in $\mathbf{d}_r$, yellow solid circles denotes the data symbols in $\mathbf{d}_s$, and red solid circles denotes the elements allocated in $[\mathbf{d}]_{\mathcal{J}}$.

ence during the pilot generation for any block transmission system with modulation matrix $\mathbf{A}$, leading to a significant improvement in LMMSE channel estimation accuracy compared to the conventional methods [8–10]. By (3.18) the precoder $\mathbf{S}$ and $\mathbf{T}$ could be exactly determined when the modulation matrix $\mathbf{A}$, pilot-stone indexes $\mathcal{Q}$, pilot-hole indexes $\mathcal{J}$, and the data-hole indexes $\mathcal{I}$ are given. The number of pilot-stone indexes $|\mathcal{Q}| = p$, consistent with the number of the corresponding pilot symbols, are recommended to be set greater than the channel length N for acceptable channel estimation performance. With a appropriate index choice, the interference-cancellation precoder for any $D \times D$ modulation matrix $\mathbf{A}$ could be obtained.

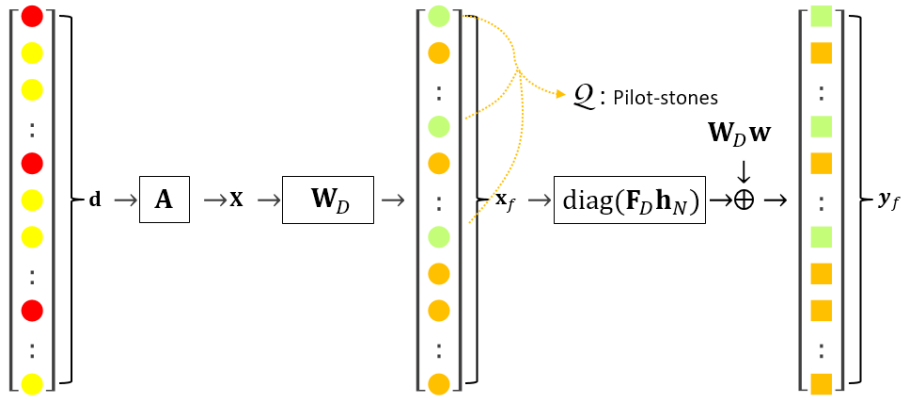

Figure 3.4: Pilot in Frequency Domain: The transmit symbols in frequency domain $\mathbf{x}_f = \mathbf{W}_D\mathbf{x}$ are denoted by green circles(called "**pilot-stones**") and orange circles.

doi:10.6342/NTU201902242

3.4 Index Choice for GFDM

For our proposed precoder (3.18), the pilot-stone indexes $\mathcal{Q} \subset \{0, 1, ..., D-1\}$, pilot-hole indexes $\mathcal{J} \subset \{0, 1, ..., D-1\}$, and data-hole indexes $\mathcal{I} \subset \{0, 1, ..., D-1\}$ determine the final form of precoder. In most cases, the channel length $N \leq K$ and we could use $p = K$ pilots for channel estimation. For channel length $N > K$ case, one could consider to use $|\mathcal{Q}| = |\mathcal{J}| = p = 2K$, where $\mathcal{Q}, \mathcal{J}$ mentioned above should be chosen such that the matrix $[\mathbf{W}_D\mathbf{A}]_{\mathcal{Q},\mathcal{J}}$ is invertible. Based on the pilots number K, we provide an appropriate indexes choice here for GFDM.

3.4.1 Pilot-stones Indexes

The indexes in the set $\mathcal{Q}$ are chosen to determine which elements in frequency-domain symbol vector $\mathbf{x}_f = \mathbf{W}_D\mathbf{A}\mathbf{d}$ would be fixed. In Fig. 3.4 the elements in fixed $[\mathbf{x}_f]_\mathcal{Q}$ are pilot-stones (green circle), and each of them is corresponding to a single OFDM subchannel. In OFDM, pilots are uniformly scattered in data block [14], that is $[\mathbf{d}]_Q = \mathbf{d}_r$. In our proposed method, the estimation is similar to OFDM where the OFDM subchannels corresponding to the fixed pilot-stones could be obtained in receiver without interference, so we select $\mathcal{Q} = \{0, D/p, 2D/p, ..., (p-1)D/p\}$, where p is the number of pilot stones. When K pilots are used for channel estimation, we could choose $\mathcal{Q} = \{0, M, M, 3M, ..., (K-1)M\}$, where $p = |\mathcal{Q}| = K$.

3.4.2 Pilot-holes and Data-holes Indexes

The pilot-holes and data-holes indexes are indexed by $\mathcal{J}$ and $\mathcal{I}$. A GFDM modulation matrix $\mathbf{A}$ (2.1) has a block-circularly structure between subsymbols, which gives the property that

$$\begin{aligned} &[\mathbf{W}_D\mathbf{A}]_{\mathcal{Q},\{0,1,...,K-1\}} = [\mathbf{W}_D\mathbf{A}]_{\mathcal{Q},\{K,K+1,...,2K-1\}} = ... \\ &[\mathbf{W}_D\mathbf{A}]_{\mathcal{Q},\{(M-1)K,(M-1)K+1,...,D-1\}}, \mathcal{Q} = \{0, M, 2M, ..., (K-1)M\}. \end{aligned} \tag{3.19}$$

doi:10.6342/NTU201902242

For $\mathcal{Q} = \{0, M, M, 3M, ..., (K-1)M\}$, the matrices $[\mathbf{W}_D\mathbf{A}]_{\mathcal{Q},\{mK,mK+1,...,mK+K-1\}}$ indexed by subsymbols $m = 0, 1...M-1$ are exactly identical. We propose a indexes choice for pilot-holes and data-holes, where

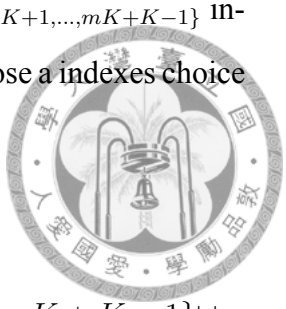

$$\begin{aligned}
&\mathcal{J} = \{m_1K, m_1K+1, ..., m_1K+K-1\},\\
&\mathcal{I} = \{m_2K, m_2K+1, ..., m_2K+K-1\} \cup \{m_3K, m_3K+1, ..., m_3K+K-1\} \cup\\
&\{m_4K, m_4K+1, ..., m_4K+K-1\} \cup ...\{m_MK, m_MK+1, ..., m_MK+K-1\},\\
&m_1, m_2, m_3, m_M... \in \{0, 1, 2, ..., M-1\}, m_1 \neq m_2 \neq m_3 \neq ...m_M.
\end{aligned} \tag{3.20}$$

The indexes set $\mathcal{J}$ is used for pilot-holes, and $\mathcal{I}$ is the data-holes indexes set. The set $\mathcal{J}$ allocates the subsymbol m_1 for pilot-holes and $\mathcal{I}$ allocates m_2,m_3,...m_M for data-holes. By choosing $m_1 = 0$, $\{m_2, m_3, ...m_M\} = \{1, 2, ...M-1\}$ and substituting (3.20) into (3.18) , the proposed **S**, **T** solution for GFDM can be derived

$$\begin{aligned}
&\mathbf{S} = [\mathbf{I}_D]_{:,\mathcal{J}}([\mathbf{W}_D\mathbf{A}]_{\mathcal{Q},\mathcal{J}})^{-1}\\
&= \begin{bmatrix} ([\mathbf{W}_D\mathbf{A}]_{\mathcal{Q},\{0,1,...,K-1\}})^{-1} \\ \mathbf{O}_{D-K,K} \end{bmatrix},\\
&\mathbf{T} = [\mathbf{I}_D]_{:,\{K,K+1,...,D-1\}} - [\mathbf{I}_D]_{:,\{0,1,2,...,K-1\}}([\mathbf{W}_D\mathbf{A}]_{\mathcal{Q},\{0,1,...,K-1\}})^{-1}[\mathbf{W}_D\mathbf{A}]_{\mathcal{Q},\{0,1,...,K-1\}} \underbrace{[\mathbf{I}_K...\mathbf{I}_K]}_{M-1}\\
&= [\mathbf{I}_D]_{:,\{K,K+1,...,D-1\}} - [\mathbf{I}_D]_{:,\{0,1,2,...,K-1\}} \underbrace{[\mathbf{I}_K...\mathbf{I}_K]}_{M-1}\\
&= \begin{bmatrix} -\overbrace{[\mathbf{I}_K...\mathbf{I}_K]}^{M-1} \\ \mathbf{I}_{D-K} \end{bmatrix}, \mathcal{Q} = \{0, M, 2M, ..., (K-1)M\}.
\end{aligned} \tag{3.21}$$

Notice that for given $\mathcal{Q} = \{0, M, 2M, ..., (K-1)M$, the choices of $\mathcal{J}$,$\mathcal{I}$ have to make $([\mathbf{W}_D\mathbf{A}]_{\mathcal{Q},\mathcal{J}})^{-1}$ exists, and different choices of $\mathcal{J}$,$\mathcal{I}$ do not affect the channel estimation performance. Considering the additional computational complexity for pilot-insertion, the precoder **T** in (3.21) does not need any multiplier and **S** corresponding to $\mathbf{d}_r$ determine the precoded pilot vector $\mathbf{d}_p = \mathbf{S}\mathbf{d}_r$, only need a one-time $O(K^3)$ computation which is negligible.

doi:10.6342/NTU201902242

3.5 IFPI-GFDM Channel Estimation

The pilot-insertion precoder in (3.18) guarantees an idea channel estimation performance without interference for a modulation matrix $\mathbf{A}$, and $\mathbf{A}$ could be any $D \times D$ matrix. Interference-free pilots insertion (IFPI-GFDM) [15] modify the original GFDM modulation matrix $\mathbf{A}$ where specific pilot symbols in data block would not be interfered by data symbols. IFPI-GFDM is based on the frequency-domain implementation [15]. In this section, we explain the frequency-domain implementation of GFDM and express the IFPI-GFDM with a modified modulation matrix $\mathbf{A}_{IFPI}$. We will also show our proposed pilot-insertion precoder for IFPI-GFDM matrix $\mathbf{A}_{IFPI}$.

3.5.1 The Frequency-Domain Implementation for GFDM

When the data block $\mathbf{d}$ is permutated with a permutation matrix $\mathbf{P}_\pi$, denoted as $\mathbf{d}_\pi = \mathbf{P}_\pi \mathbf{d}$, the transmit symbol vector $\mathbf{x}$ could be equivalently expressed by $\mathbf{d}_\pi$ as

$$\mathbf{x} = \mathbf{A}\mathbf{d} = \mathbf{A}\mathbf{P}_\pi^T \mathbf{P}_\pi \mathbf{d} = \mathbf{A}_\pi \mathbf{d}_\pi,$$

where $\mathbf{A}_\pi = \mathbf{A}{\mathbf{P}_\pi}^T$ is a column-permutated GFDM matrix with $[\mathbf{A}_\pi]_{:,m+kM} = [\mathbf{A}]_{:,k+mK}$ and $\mathbf{d}_\pi = \mathbf{P}_\pi \mathbf{d}$ is a permutated data vector with $[\mathbf{d}_\pi]_{m+kM} = [\mathbf{d}]_{k+mK}$. The permutation matrix $\mathbf{P}_\pi$ could be defined as

$$\mathbf{P}_\pi = [\mathbf{C}_0[\mathbf{I}_D]_{:,0,M,2M,\ldots,(K-1)M}, \mathbf{C}_1[\mathbf{I}_D]_{:,0,M,2M,\ldots,(K-1)M}, \ldots, \mathbf{C}_{M-1}[\mathbf{I}_D]_{:,0,M,2M,\ldots,(K-1)M}],$$

where the submatrix $\mathbf{C}_m[\mathbf{I}_D]_{:,0,M,2M,\ldots,(K-1)M}$ contains a $D \times D$ m-points circular shift matrix $\mathbf{C}_m = \begin{bmatrix} [\mathbf{I}_D]_{\langle m \rangle_D,:} \\ [\mathbf{I}_D]_{\langle m+1 \rangle_D,:} \\ \cdots \\ [\mathbf{I}_D]_{\langle m+(D-1) \rangle_D,:} \end{bmatrix}$ and a allocating matrix $[\mathbf{I}_D]_{:,0,M,2M,\ldots,(K-1)M}$. The

doi:10.6342/NTU201902242

permutated GFDM matrix $\mathbf{A}_\pi$ could be equivalently expressed as [15]

$$\mathbf{A}_\pi = \mathbf{W}_D^H \mathbf{G}_R \,\text{blkdiag}(\underbrace{\mathbf{W}_M, ..., \mathbf{W}_M}_{K}), \tag{3.22}$$

where

$$\mathbf{G}_R = [\mathbf{C}_0 \,\text{diag}(\mathbf{W}_D\mathbf{g})\mathbf{R},\ \mathbf{C}_M \,\text{diag}(\mathbf{W}_D\mathbf{g})\mathbf{R},\ ...,\ \mathbf{C}_{(K-1)M} \,\text{diag}(\mathbf{W}_D\mathbf{g})\mathbf{R}]$$

and $\mathbf{R}$ is a repetition matrix $[\underbrace{\mathbf{I}_M, ..., \mathbf{I}_M}_{K}]^T$. The implementation in (3.22) ending with an IDFT is so-called frequency-domain implementation. The $\mathbf{W}_D\mathbf{g}$ part in matrix $\mathbf{G}_R$ is the prototype vector in frequency domain.

3.5.2 The Modulation Matrix for IFPI-GFDM

The IFPI-GFDM matrix is modified from (3.22) to be

$$\mathbf{A}_{IFPI} = \mathbf{W}_D^H \mathbf{G}_R \,\text{blkdiag}(\underbrace{\Gamma, ..., \Gamma}_{K}), \tag{3.23}$$

and in [15] SISO case $\Gamma = \mathbf{P}_\pi{}' \,\text{blkdiag}(\lambda_1, \lambda_2\mathbf{W}_{M-1})$ is an alternative to original M-point DFT matrix $\mathbf{W}_M$, where $\mathbf{P}_\pi{}'$ permutates the pilots. As an example, we set $\mathbf{P}_\pi{}' = \mathbf{I}_M$ and use the Dirichlet protypefilter whose $\mathbf{G}_R$ is identity matrix $\mathbf{I}_D$. We could get

$$\mathbf{A}_{IFPI} = \mathbf{W}_D^H \,\text{blkdiag}(\underbrace{\Gamma, ..., \Gamma}_{K}), \tag{3.24}$$

where $\Gamma = \text{blkdiag}(\lambda_1, \lambda_2\mathbf{W}_{M-1})$ and the parameter λ_1,λ_2 are scaling factors that normalize the carriers power. Obviously, the K column vectors in submatrix $[\mathbf{A}_{IFPI}]_{:,0,M,2M,3M,...(K-1)M} = [\mathbf{W}_D^H]_{:,0,M,2M,3M,...(K-1)M}$ are equal to the OFDM subcarriers which could guarantee at most K pilot symbols in data block $\mathbf{d}$ to be interference-free.

doi:10.6342/NTU201902242

3.5.3 The Proposed Pilot-insertion Precoder for IFPI-GFDM

We substitute $\mathbf{A} = \mathbf{A}_{IFPI}\mathbf{P}_\pi$ into (3.18) and select $\mathcal{Q} = \{0, M, 2M, ..., (K-1)M\}$, $\mathcal{J} = \{0, 1, 2, ..., K-1)\}$, $\mathcal{I} = \{K, K+1, ..., (D-1)\}$ to derive the proposed precoder for IFPI-GFDM. We could get

$$[\mathbf{W}_D\mathbf{A}]_{\mathcal{Q},\mathcal{I}} = \mathbf{O}_{p,d}. \tag{3.25}$$

and

$$[\mathbf{W}_D\mathbf{A}]_{\mathcal{Q},\mathcal{J}} = \lambda_1[\mathbf{G}_R]_{\mathcal{Q},\mathcal{Q}} = \mathbf{I}_p. \tag{3.26}$$

Proof. We first derive

$$\begin{aligned}
[\mathbf{W}_D\mathbf{A}]_{\mathcal{Q},\mathcal{I}} &= [\mathbf{G}_R \,\text{blkdiag}(\underbrace{\Gamma, ..., \Gamma}_{K})\mathbf{P}_\pi]_{\mathcal{Q},\mathcal{I}} \\
&= [\mathbf{I}_D]_{\mathcal{Q},:}\mathbf{G}_R \,\text{blkdiag}(\underbrace{\Gamma, ..., \Gamma}_{K})\mathbf{P}_\pi[\mathbf{I}_D]_{:,\mathcal{I}} \\
&= [\mathbf{G}_R]_{\mathcal{Q},:}[\text{blkdiag}(\underbrace{\Gamma, ..., \Gamma}_{K})\mathbf{P}_\pi]_{:,\mathcal{I}} \\
&= [\mathbf{G}_R]_{\mathcal{Q},\mathcal{J}}[\text{blkdiag}(\underbrace{\Gamma, ..., \Gamma}_{K})\mathbf{P}_\pi]_{\mathcal{J},\mathcal{I}} + [\mathbf{G}_R]_{\mathcal{Q},\mathcal{I}}[\text{blkdiag}(\underbrace{\Gamma, ..., \Gamma}_{K})\mathbf{P}_\pi]_{\mathcal{I},\mathcal{I}},
\end{aligned} \tag{3.27}$$

where $[\text{blkdiag}(\underbrace{\Gamma, ..., \Gamma}_{K})\mathbf{P}_\pi]_{\mathcal{J},\mathcal{I}} = \mathbf{O}_{p,d}$ and $[\mathbf{G}_R]_{\mathcal{Q},\mathcal{I}} = \mathbf{O}_{p,d}$ are zero matrices. We get

$$[\mathbf{W}_D\mathbf{A}]_{\mathcal{Q},\mathcal{I}} = \mathbf{O}_{p,d}. \tag{3.28}$$

Similarly, we could derive

$$\begin{aligned}
&[\mathbf{W}_D\mathbf{A}]_{\mathcal{Q},\mathcal{J}} = [\mathbf{G}_R]_{\mathcal{Q},\mathcal{Q}}[\text{blkdiag}(\underbrace{\Gamma, ..., \Gamma}_{K})\mathbf{P}_\pi]_{\mathcal{Q},\mathcal{J}} + [\mathbf{G}_R]_{\mathcal{Q},\{\mathcal{D}-\mathcal{Q}\}} \cdot \\
&[\text{blkdiag}(\underbrace{\Gamma, ..., \Gamma}_{K})\mathbf{P}_\pi]_{\{\mathcal{D}-\mathcal{Q}\},\mathcal{J}}, \mathcal{D} = \{0, 1, 2, ...D-1\},
\end{aligned} \tag{3.29}$$

doi:10.6342/NTU201902242

where $[\text{blkdiag}(\underbrace{\Gamma, ..., \Gamma}_{K})\mathbf{P}_{\pi}]_{\mathcal{Q},\mathcal{J}} = \lambda_1 \mathbf{I}_p$ and $[\mathbf{G}_R]_{\mathcal{Q},\{\mathcal{D}-\mathcal{Q}\}} = \mathbf{O}_{p,d}$. We get

$$[\mathbf{W}_D\mathbf{A}]_{\mathcal{Q},\mathcal{J}} = \lambda_1 [\mathbf{G}_R]_{\mathcal{Q},\mathcal{Q}} = \mathbf{I}_p. \tag{3.30}$$

□

The proposed precoder for IFPI-GFDM is derived as

$$\mathbf{S} = [\mathbf{I}_D]_{:,\mathcal{J}}, \mathbf{T} = [\mathbf{I}_D]_{:,\mathcal{I}}, \tag{3.31}$$

which is consistent with the conventional pilot-insertion, this show why IFPI-GFDM could claim itself interference-free only using a conventional pilot-insertion. The Fig. 3.5 indi-

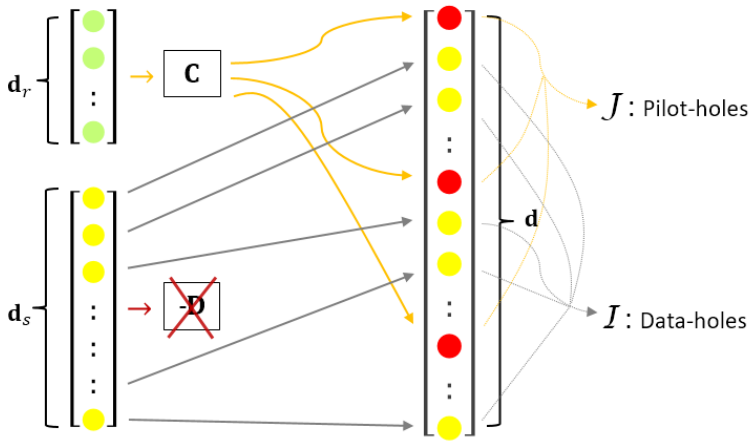

Figure 3.5: Pilot-insertion for IFPI-GFDM

cates that for this kind of modulation matrices like IFPI-GFDM, OFDM, etc, the precoding matrix **D** for data symbols is trivial, and the additional transmit power for pilot-insertion precoder could be saved dramatically. Notice that in SISO case IFPI-GFDM could only guarantee K pilot symbols to be interference-free, and for this method the subcarriers number K could not be set too small.

doi:10.6342/NTU201902242

Chapter 4

Simulation Results

In this section, numerical results are presented to compare the performances of the conventional methods [8–10] with the proposed method for GFDM and IFPI-GFDM, in terms of mean square error (MSE) of LMMSE channel estimation and symbol error rate (SER). Both the Dirichlet [16] and raised cosine (RC) [1] filters are employed as our prototype filter. In addition, OFDM channel estimation is included in the experiments for a comprehensive comparison.

4.1 Parameter Settings

The modulation is QPSK, the symbol energy is $E_s = 1$, the equalizer is the zero-forcing equalizer, and the roll-off factor of the RC filter is $\alpha = 0.5$. We consider two cases $(K, M) = (16, 8)$ and $(8, 16)$ for GFDM. For a fair comparison, the same block size is used for OFDM, i.e., $(K, M) = (128, 1)$. The channel length is $N = D/8 = 16$, and the pilot number is set to be $p = 16$. The pilot-stones indexes set is $\mathcal{Q} = \{0, 8, 16, ..., 120\}$ and the pilot-holes indexes set is $\mathcal{J} = \{0, 1, 2, ..., 15\}$. To evaluate the performances, Monte Carlo simulation is adopted with randomly generated channel realizations and independent data sets for the realizations. We generate $N_h = 100$ spatially Rayleigh fading channel realizations, whose channel PDP is exponential from 0 to -10 dB with N taps, and $N_d = 100$ independent data blocks for each channel realization. Moreover, the genie-aided condition, where full CSI is known, is included and considered as the performance

doi:10.6342/NTU201902242

bound for the SER evaluation of all schemes.

4.1.1 Simulation Results

For the case $(K, M) = (16, 8)$, the simulation results are shown in Fig. 4.1. With Dirichlet prototype filter in Fig. 4.1(a), the MSE is calculated by averaging through the pairwise Euclidean norms between a channel realization and its LMMSE estimated counterpart. According to Fig. 4.1(a), the proposed method significantly outperforms the conventional methods, especially under high SNR where the impact of interference is much larger than that of noise, since the proposed method precancels the effect of interference during pilot generation. The IFPI-GFDM could get the same performance as OFDM by interference-free pilot-insertion, where our proposed precoder in this case also get the best performance.

When we interpret the SER performance presented in Fig. 4.1(b), it can be observed that the proposed method outperforms the conventional methods under high SNR but performs comparably to the conventional methods under low SNR since the additionally energy consumption of the pilot-insertion precoder which could relatively takes away the transmit power for data symbols and degrades SER performance. The figures 4.1(c) and 4.1(d) show the performance for GFDM with RC prototype filter, the simulation results demonstrate the similar trends with Dirichlet, but RC filter has been proved in [3] that the modulation matrix is not unitary and cause the noise enhancement.

For the case $(K, M) = (8, 16)$, the simulation results are shown in Fig. 4.2. According to Fig. 4.2(a) with Dirichlet filter, the proposed method significantly outperforms the conventional methods, especially under high SNR where the impact of interference is much larger than that of noise, since the proposed method precancels the effect of interference during pilot generation. However, the IFPI-GFDM with the conventional pilot-insertion could not performs the best among all schemes anymore, because the existing IFPI-GFDM in SISO case [11] could only provide one pilot symbol within per subsymbol and at most K pilot symbols for whole transmit block to guarantee the interference-free pilot-insertion and the channel length of $N = 2K$ exceeds the limit. In the other hand, our proposed precoder has no limit to precanceling the effect of interference during pilot

doi:10.6342/NTU201902242

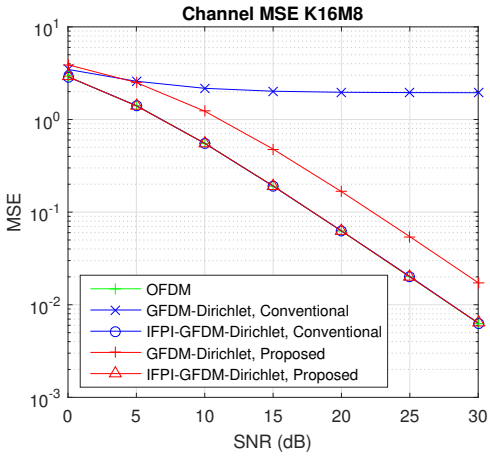

(a) Channel MSE, Dirichlet

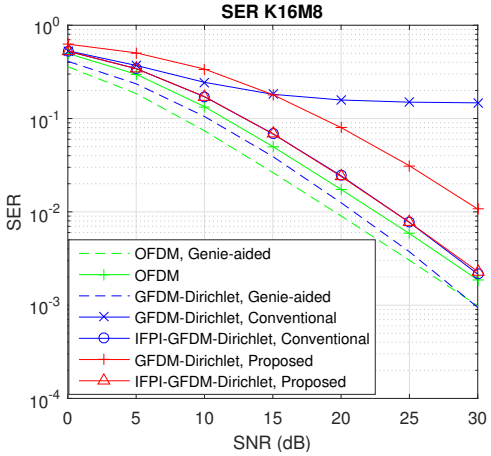

(b) SER, Dirichlet

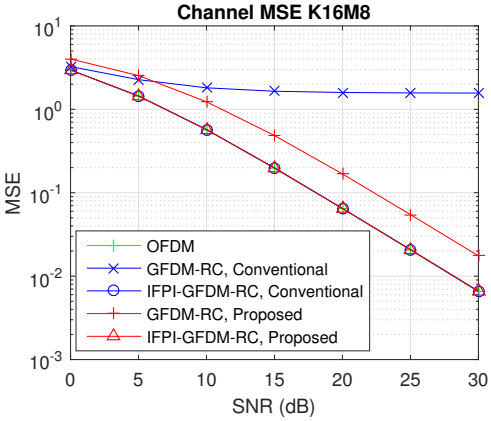

(c) Channel MSE, RC

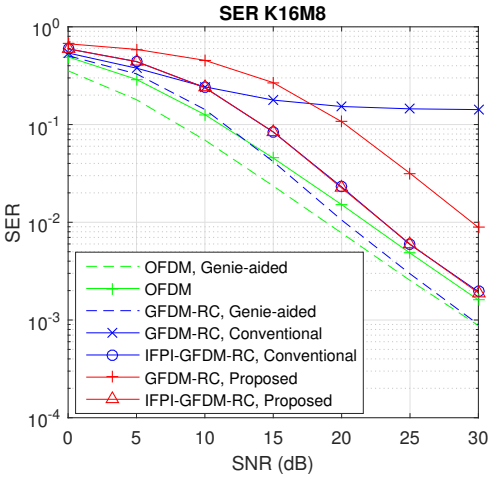

(d) SER, RC

Figure 4.1: Performance Comparison for $K = 16, M = 8$

doi:10.6342/NTU201902242

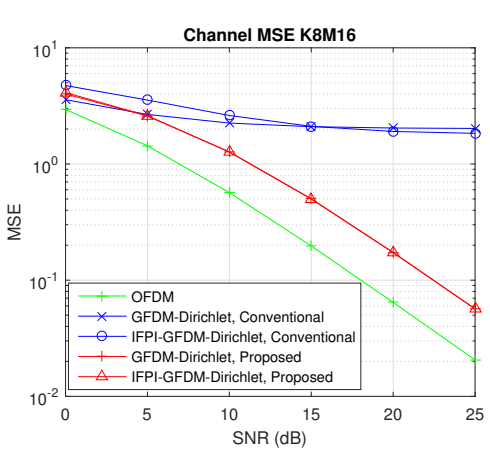

(a) Channel MSE, Dirichlet

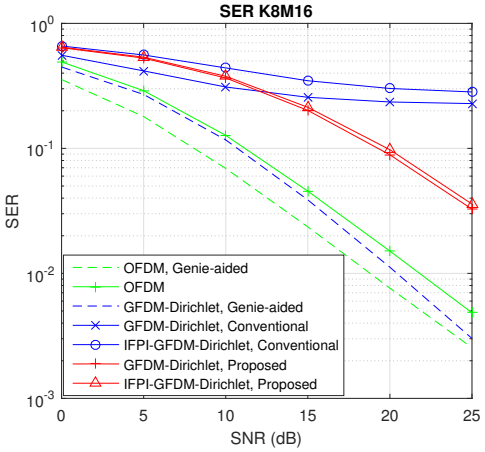

(b) SER, Dirichlet

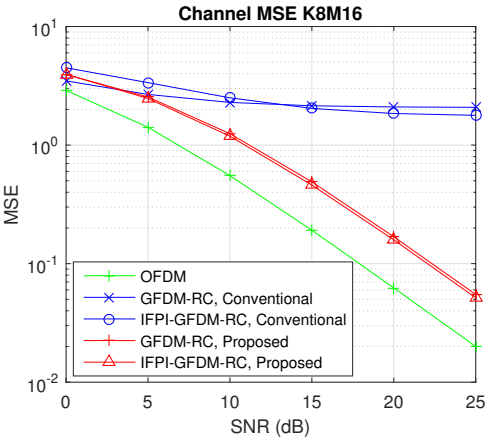

(c) Channel MSE, RC

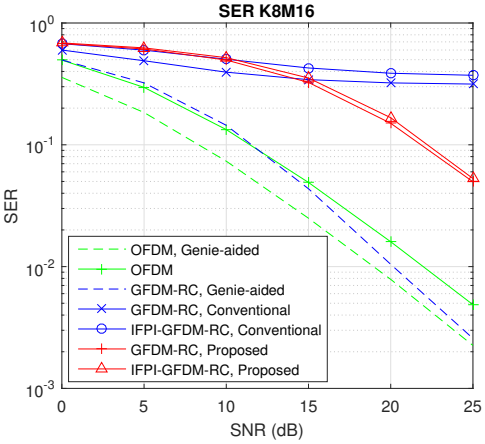

(d) SER, RC

Figure 4.2: Performance Comparison for $K = 8, M = 16$

generation. When we interpret the SER performance presented in Fig. 4.2(b), it can be observed that the proposed method outperforms the conventional methods under high SNR and performs comparably to the conventional methods under low SNR. The IFPI-GFDM with the conventional pilot-insertion could not performs well due to the channel estimation performance degradation. Our proposed method could outforms the conventional methods for both GFDM and IFPI GFDM, but OFDM still performs the best among all schemes, with its performance gap between the curves of LMMSE channel estimation and genie-aided scheme smaller than that of GFDM. The figures 4.2(c) and 4.2(d) show the performance for GFDM with RC prototype filter, the simulation results demonstrate the similar trends and RC filter cause the noise enhancement at low SNR.

doi:10.6342/NTU201902242

Chapter 5

Conclusion

In this thesis, a general pilot-insertion precoding technique for generalized frequency division multiplexing (GFDM), as well as any other block-based communication systems, is formulated. The corresponding linear minimum mean square error (LMMSE) channel estimator is also derived. A condition that guarantees cancellation of interference for pilot-aided channel estimation commonly present in GFDM systems is defined. The condition is called "pilot-stone condition" and requires the transmit samples at selected frequency bins (i.e., pilot-stones) to be a fixed reference sequence. A procedure is proposed to find a solution for the GFDM precoder to satisfy the pilot-stone condition, where the proposed precoder with proper indexes choice could be low-complexity and there is no need for receiver to cancel the channel estimation interference. Simulation results demonstrate that for original GFDM, our proposed method outperforms the conventional methods in channel MSE under high SNR where the impact of interference is much larger than that of noise, and the proposed method precancels the effect of interference during pilot generation. The proposed pilot-insertion precoder could be viewed as a generalized version of the so-called interference-free pilot-insertion (IFPI) GFDM [11]. In the future, it is desirable to identify the class of GFDM precoders that simultaneously satisfy the properties of interference-free channel estimation, low out-of-band emission, and low-complexity implementation. As illustrated in Figure 5.1, a comprehensive waveform precoder based on our findings are still yet to be researched.

doi:10.6342/NTU201902242

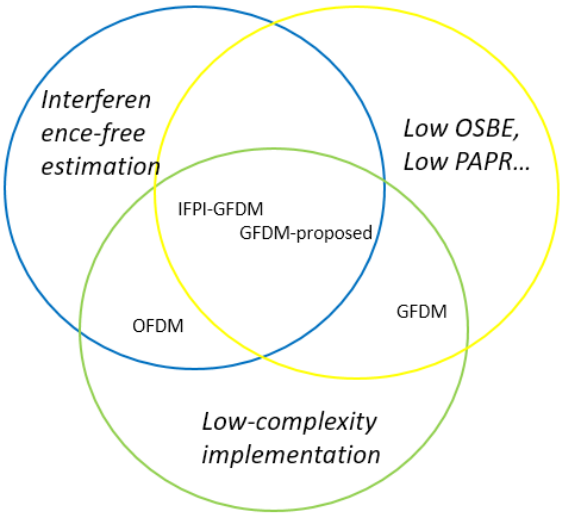

Figure 5.1: Future Work

doi:10.6342/NTU201902242

Bibliography

[1] N. Michailow, M. Matthé, I.S. Gaspar, A.N. Caldevilla, L.L. Mendes, A. Festag, and G. Fettweis. Generalized frequency division multiplexing for 5th generation cellular networks. *IEEE Transactions on Communications*, 62(9):3045–3061, Sept 2014.

[2] D. Zhang, L. L. Mendes, M. Matthé, I. S. Gaspar, N. Michailow, and G. P. Fettweis. Expectation propagation for near-optimum detection of mimo-gfdm signals. *IEEE Transactions on Wireless Communications*, 15(2):1045–1062, Feb 2016.

[3] P. C. Chen, B. Su, and Y. Huang. Matrix characterization for gfdm: Low complexity mmse receivers and optimal filters. *IEEE Transactions on Signal Processing*, 65(18):4940–4955, Sept 2017.

[4] U. Vilaipornsawai and M. Jia. Scattered-pilot channel estimation for GFDM. In *2014 IEEE Wireless Commun. and Networking Conf. (WCNC)*, pages 1053–1058, April 2014.

[5] M. Danneberg, N. Michailow, I. Gaspar, M. Matthé, Dan Zhang, L. L. Mendes, and G. Fettweis. Implementation of a 2 by 2 MIMO-GFDM transceiver for robust 5G networks. In *2015 Int. Symposium on Wireless Communication Systems (ISWCS)*, pages 236–240, Aug 2015.

[6] J. Zhang, Y. Li, and K. Niu. Iterative channel estimation algorithm based on compressive sensing for GFDM. In *2016 IEEE International Conference on Network Infrastructure and Digital Content (IC-NIDC)*, pages 244–248, Sept 2016.

doi:10.6342/NTU201902242

[7] Shahab Ehsanfar, Maximilian Matthé, Marwa Chafii, and Gerhard Fettweis. Pilot- and cp-aided channel estimation in mimo non-orthogonal multi-carriers. *IEEE Transactions on Wireless Communications*, PP:1–1, 12 2018.

[8] S. Ehsanfar, M. Matthé, D. Zhang, and G. Fettweis. A Study of Pilot-Aided Channel Estimation in MIMO-GFDM Systems. In *WSA 2016; 20th Int. ITG Workshop on Smart Antennas*, pages 1–8, March 2016.

[9] S. Ehsanfar, M. Matthe, D. Zhang, and G. Fettweis. Theoretical Analysis and CRLB Evaluation for Pilot-Aided Channel Estimation in GFDM. In *2016 IEEE Global Communications Conference (GLOBECOM)*, pages 1–7, Dec 2016.

[10] Y. Akai, Y. Enjoji, Y. Sanada, R. Kimura, H. Matsuda, N. Kusashima, and R. Sawai. Channel estimation with scattered pilots in GFDM with multiple subcarrier bandwidths. In *2017 IEEE 28th Annual International Symposium on Personal, Indoor, and Mobile Radio Communications (PIMRC)*, pages 1–5, Oct 2017.

[11] S. Ehsanfar, M. Matthe, D. Zhang, and G. Fettweis. Interference-Free Pilots Insertion for MIMO-GFDM Channel Estimation. In *2017 IEEE Wireless Communications and Networking Conference (WCNC)*, pages 1–6, March 2017.

[12] Marc Moonen. Block transmission techniques for wireless communications block transmission techniques for wireless communications. 2004.

[13] A. Hjorungnes and D. Gesbert. Complex-valued matrix differentiation: Techniques and key results. *IEEE Transactions on Signal Processing*, 55(6):2740–2746, June 2007.

[14] Yuan-Pei Lin, See-May Phoong, and P. P. Vaidyanathan. *Filter Bank Transceivers for OFDM and DMT Systems*. Cambridge University Press, New York, NY, USA, 2010.

[15] S. Ehsanfar, M. Matthe, D. Zhang, and G. Fettweis. Interference-free pilots insertion for mimo-gfdm channel estimation. In *2017 IEEE Wireless Communications and Networking Conference (WCNC)*, pages 1–6, March 2017.

doi:10.6342/NTU201902242

[16] M. Matthé, N. Michailow, I. Gaspar, and G. Fettweis. Influence of pulse shaping on bit error rate performance and out of band radiation of Generalized Frequency Division Multiplexing. In *Proc. IEEE ICC Workshop*, pages 43–48, 2014.

doi:10.6342/NTU201902242

Appendix A

Power Spectral Density

By passing $x[n]$ through a D/A converter with a sampling interval T_s and an interpolation filter $p(t)$, the analog baseband transmit signal $x_a(t)$ is obtained, i.e.,

$$x_a(t) = \sum_{n=-\infty}^{\infty} x[n]p(t - nT_s).$$

In modern digital-signal-processing-based communication systems [14], we consider that if $x[n]$ is a CWSS process, the power spectral density(PSD) of $x_a(t)$ can be obtained as

$$S_a(f) = \frac{1}{T_s} S_x(e^{j2\pi f T_s})|P(f)|^2, \tag{A.1}$$

where $S_x(e^{j(\omega=2\pi f T_s)})$ is the average PSD of a CWSS process $x[n]$ and $P(f)$ is the Fourier transform of an interpolation filter.

A.1 For Original GFDM

Theorem 2. *Given a $D \times D$ GFDM modulation matrix* **A***, the power spectral density could be expressed as*

$$S_a(f) = \frac{E_s|P(f)|^2}{DT_s} \sum_{k\in\mathcal{K}} \sum_{m\in\mathcal{M}} |G_m(e^{j(\omega-2\pi k/K)})|^2, \tag{A.2}$$

doi:10.6342/NTU201902242

where

$$g_m[n] = \begin{cases} [\mathbf{g}]_{\langle n-mK\rangle_D}, & n = 0, 1, ..., D-1 \\ 0, & \textit{otherwise} \end{cases}, \tag{A.3}$$

and $G_m(e^{j\omega}) = \text{DTFT}_n\ (g_m[n])$.

A expression with the GFDM matrix in frequency domain $\mathbf{P} = \mathbf{W}_D\mathbf{A}$ is

$$S_a(f) = \frac{E_s|P(f)^2|}{DT_s} \sum_{k=0}^{K-1} \sum_{m=0}^{M-1} |P_{m,k}(e^{j2\pi f T_s})|^2, \tag{A.4}$$

where

$$P_{m,k}(e^{j\omega}) = \sum_{l=0}^{D-1} [\mathbf{P}]_{l,m+kM} \mathcal{S}(\omega - \frac{2\pi l}{D}), \tag{A.5}$$

$\mathcal{S}(\omega) = sinc_D(\omega)e^{-j\omega\frac{D-1}{2}}$, and $sinc_D(x)$ is the periodic sinc function.

Proof of Theorem 2. □

For the equation (2.3) and the CP length $L = 0$, we could obtain the transmit signal in GFDM

$$x[n] = \sum_{l=-\infty}^{\infty} \sum_{k\in\mathcal{K}} \sum_{m\in\mathcal{M}} [\mathbf{d}_l]_{m+kM} g_m[n - lD] e^{j2\pi k(n-lD)/K}, \tag{A.6}$$

where

$$g_m[n] = \begin{cases} [\mathbf{g}]_{\langle n-mK\rangle_D}, & n = 0, 1, ..., D-1 \\ 0, & \text{otherwise} \end{cases}. \tag{A.7}$$

The average autocorrelation function[1] of $x[n]$ can be expressed as

$$R_x[i] = \frac{1}{D} \sum_{n=0}^{D-1} \text{E}\{x[n]x^*[n-i]\}, \tag{A.8}$$

Substituting (A.6) into (A.8), we can obtain

$$\begin{aligned} R_x[i] \;=\; & \frac{1}{D} \sum_{n=0}^{D-1} \text{E} \Bigg\{ \sum_{l=-\infty}^{\infty} \sum_{l'=-\infty}^{\infty} \sum_{k\in\mathcal{K}} \sum_{k'\in\mathcal{K}} \sum_{m\in\mathcal{M}} \sum_{m'\in\mathcal{M}} [\mathbf{d}_l]_{m+kM} [\mathbf{d}_{l'}]^*_{m'+k'M} \\ & \cdot g_m[n - lD] g^*_{m'}[n - i - l'D] e^{j2\pi k(n-lD)/K} e^{-j2\pi k'(n-i-l'D)/K} \Bigg\}. \end{aligned} \tag{A.9}$$

[1] as defined in [14], P.331,

doi:10.6342/NTU201902242

Now, because

$$\mathrm{E}\{[\mathbf{d}_l]_{m+kM}[\mathbf{d}_{l'}]^*_{m'+k'M}\} = \begin{cases} E_s, & l=l', k=k', m=m' \\ 0, & \text{otherwise} \end{cases}, \tag{A.10}$$

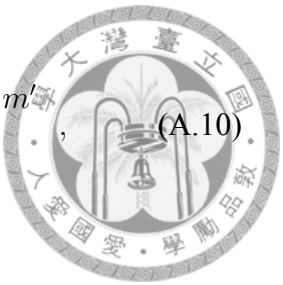

we could get

$$R_x[i] = \frac{E_s}{D}\sum_{n=0}^{D-1}\sum_{l=-\infty}^{\infty}\sum_{k\in\mathcal{K}}\sum_{m\in\mathcal{M}} \tag{A.11}$$

$$\mathrm{E}\{g_m[n-lD]g_m^*[n-i-lD]e^{j2\pi k(n-lD)/K}e^{-j2\pi k(n-i-lD)/K}\}. \tag{A.12}$$

$$= \frac{E_s}{D}\sum_{n=0}^{D-1}\sum_{l=-\infty}^{\infty}\sum_{k\in\mathcal{K}}\sum_{m\in\mathcal{M}} g_m[n-lD]g_m^*[n-i-lD]e^{j2\pi ki/K}. \tag{A.13}$$

From (A.6), where $g_m[n-lD]=0$ if $n-lD \notin \{0,1,...,D-1\}$, that is,

$$g_m[n-lD]=0, l \notin \{1,...,D-1\},$$

we can derive that

$$R_x[i] = \frac{E_s}{D}\sum_{n=0}^{D-1}\sum_{k\in\mathcal{K}}\sum_{m\in\mathcal{M}} g_m[n]g_m^*[n-i]e^{j2\pi ki/K}. \tag{A.14}$$

By [14], we define the average power spectrum of a CWSS process as the Discrete-time Fourier transform(DTFT) of the average auto-correlation function

$$S_x(e^{j\omega}) = \sum_{k=-\infty}^{\infty} R_x[k]e^{-j\omega k}. \tag{A.15}$$

For simplicity, we denote the DTFT operation as in

$$G(e^{j\omega}) = \mathrm{DTFT}_n\ (g[n])$$

doi:10.6342/NTU201902242

and (A.15) can be written as $S_x(e^{j\omega}) = \text{DTFT}_n\ (R_x[k])$

$$= \frac{E_s}{D} \sum_{n=0}^{D-1} \sum_{k\in\mathcal{K}} \sum_{m\in\mathcal{M}} g_m[n]\text{DTFT}_i\ (g_m^*[n-i]e^{j2\pi ki/K}). \tag{A.16}$$

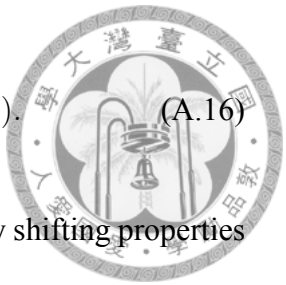

Using the time reversal, time conjugation, time shifting, and frequency shifting properties of DTFT[2], we could get

$$\text{DTFT}_i\ ((g_m^*[n-i]e^{j2\pi ki/K})) = G_m^*(e^{j(\omega-2\pi k/K)})e^{-j(\omega-2\pi k/K)n}, \tag{A.17}$$

and obtain

$$S_x(e^{j\omega}) = \frac{E_s}{D} \sum_{k\in\mathcal{K}} \sum_{m\in\mathcal{M}} (\sum_{n=0}^{D-1} g_m[n]e^{-j(\omega-2\pi k/K)n}) G_m^*(e^{j(\omega-2\pi k/K)}),$$

$$= \frac{E_s}{D} \sum_{k\in\mathcal{K}} \sum_{m\in\mathcal{M}} G_m(e^{j(\omega-2\pi k/K)}) G_m^*(e^{j(\omega-2\pi k/K)}),$$

$$= \frac{E_s}{D} \sum_{k\in\mathcal{K}} \sum_{m\in\mathcal{M}} |G_m(e^{j(\omega-2\pi k/K)})|^2. \tag{A.18}$$

By substituting (A.18) into (A.1), we finally get the power spectrum of $x_a(t)$,

$$S_a(f) = \frac{E_s|P(f)|^2}{DT_s} \sum_{k\in\mathcal{K}} \sum_{m\in\mathcal{M}} |G_m(e^{j(\omega-2\pi k/K)})|^2. \tag{A.19}$$

A.2 For General GFDM Precoder "A"

Theorem 3. *Given any $D' \times D$ modulation matrix* **A***, and $\mathcal{I}$ denotes the carriers selected in* **A***, the power spectral density could be expressed as*

$$S_a(f) = \frac{E_s|P(f)|^2}{D'T_s} \|(\mathbf{v}_{D'}(e^{j2\pi fTs})^H[\mathbf{A}']_{:,\mathcal{I}})^T\|^2. \tag{A.20}$$

[2]as defined in Wikipedia, https://en.wikipedia.org/wiki/Discrete-time_Fourier_transform

doi:10.6342/NTU201902242

Notice that for original GFDM, the equation below can be derived from (2.4) that

$$a_s[n] = g_m[n]e^{j2\pi kn/K}, s = m + kM$$

and we could get the equation by DTFT

$$\text{DTFT}_n\ (a_s[n]) = A_s(e^{j\omega}) = G_m(e^{j(\omega-2\pi k/K)}), s = m + kM. \tag{A.21}$$

Substituting (A.21) into (A.20), we get the power spectrum of $x_a(t)$,

$$S_a(f) = \frac{E_s|P(f)|^2}{DT_s}\sum_{k\in\mathcal{K}}\sum_{m\in\mathcal{M}}|G_m(e^{j(\omega-2\pi k/K)})|^2. \tag{A.22}$$

This coincides with the equation (A.2).

Proof of Theorem 3. For a general modulation matrix **A**, the lth transmit block $\mathbf{x}'_l$ is passed through a parallel-to-serial (P/S) conversion, and the digital baseband transmit signal can be expressed as

$$x[n] = [\mathbf{x}'_l]_r = [\mathbf{A}'\mathbf{d}_l]_r,$$

$$n \in \mathbb{Z}, l = \lfloor\frac{n}{D'}\rfloor \in \mathbb{Z}, r = \langle n\rangle_{D'} \in \{0, 1, ...D' - 1\}.$$

Notice that $[\mathbf{x}'_l]_r$ is the rth element of the lth transmitted block $\mathbf{x}'_l$, and $n = lD' + r$.

A random process x[n] is said to be cyclo wide sense stationary with the period M, if it satisfies the following two conditions:

$$(1)\ \mathrm{E}\{x[n + M]\} = \mathrm{E}\{x[n]\},$$

$$(2)\ \mathrm{E}\{x[n]x^*[n - k]\} = \mathrm{E}\{x[n + M]x^*[n + M - k]\}.$$

(1)Let

$$\mathrm{E}\{x[n]\} = \mathrm{E}\{[\mathbf{A}'\mathbf{d}_l]_r\} = \mathrm{E}\{[\mathbf{A}'(\mathbf{d}_{dl} + \mathbf{d}_{pl})]_r\},$$

doi:10.6342/NTU201902242

where $\mathbf{d}_{pl} = \mathbf{d}_p$ is constant in each block, so we get

$$\mathrm{E}\{x[n]\} = [\mathbf{A}'\,\mathrm{E}\{\mathbf{d}_{dl}\} + \mathbf{A}'\mathbf{d}_p]_r = [\mathbf{A}'\mathbf{d}_p]_r.$$

And we could get

$$\mathrm{E}\{x[n+D']\} = \mathrm{E}\{[\mathbf{A}'\mathbf{d}_{l+1}]_r\} = \mathrm{E}\{[\mathbf{A}'(\mathbf{d}_{d(l+1)}+\mathbf{d}_{p(l+1)})]_r\} = [\mathbf{A}'\,\mathrm{E}\{\mathbf{d}_{d(l+1)}\}+\mathbf{A}'\mathbf{d}_p]_r = [\mathbf{A}'\mathbf{d}_p]_r,$$

so (1) is satisfied.

(2)Let

$$\mathrm{E}\{x[n]x^*[n-k]\} = \mathrm{E}\{[\mathbf{A}'\mathbf{d}_l]_r[\mathbf{A}'\mathbf{d}_{l'}]_{r'}{}^*\}$$

$$= \mathrm{E}\{[\mathbf{A}']_{r,:}\mathbf{d}_l([\mathbf{A}']_{r',:}\mathbf{d}_{l'})^H\}$$

$$= [\mathbf{A}']_{r,:}\,\mathrm{E}\{\mathbf{d}_l\mathbf{d}_{l'}^H\}([\mathbf{A}']_{r',:})^H$$

and

$$\mathrm{E}\{x[n+M]x^*[n+M-k]\} = [\mathbf{A}']_{r,:}\,\mathrm{E}\{\mathbf{d}_{l+1}\mathbf{d}_{l'+1}^H\}([\mathbf{A}']_{r',:})^H,$$

if $l = l'$, then $\mathrm{E}\{\mathbf{d}_l\mathbf{d}_{l'}^H\} = \mathrm{E}\{\mathbf{d}_{l+1}\mathbf{d}_{l'+1}^H\}$;

if $l \neq l'$, then $\mathrm{E}\{\mathbf{d}_l\mathbf{d}_{l'}^H\} = \mathrm{E}\{\mathbf{d}_{l+1}\mathbf{d}_{l'+1}^H\} = \mathbf{O}_{D,D}$.

So we could find that

$$\mathrm{E}\{x[n+M]x^*[n+M-k]\} = [\mathbf{A}']_{r,:}\,\mathrm{E}\{\mathbf{d}_{l+1}\mathbf{d}_{l'+1}^H\}([\mathbf{A}']_{r',:})^H$$

$$= [\mathbf{A}']_{r,:}\,\mathrm{E}\{\mathbf{d}_l\mathbf{d}_{l'}^H\}([\mathbf{A}']_{r',:})^H = \mathrm{E}\{x[n]x^*[n-k]\}.$$

(2) is satisfied.

The data signal $x_d[n]$ can be expressed as

$$x_d[n] = [\mathbf{x}'_{dl}]_r = [\mathbf{A}'\mathbf{d}_{dl}]_r,$$

$$n \in \mathbb{Z}, l = \lfloor \frac{n}{D'} \rfloor \in \mathbb{Z}, r = \langle n \rangle_{D'} \in \{0, 1, ...D'-1\},$$

doi:10.6342/NTU201902242

where $\mathbf{A}'$ could be any transmit matrix, and we pick up the indexes $\mathcal{I} \subset \{0, 1, ..., D-1\}$ for i.i.d, zero-mean data symbols with symbol energy E_s, that is, $\mathrm{E}\{[\mathbf{d}_{dl}]_{\mathcal{I}}[\mathbf{d}_{dl}]_{\mathcal{I}}^H\} = E_s\mathbf{I}_{|\mathcal{I}|}$, $\mathrm{E}\{[\mathbf{d}_{dl}]_{\mathcal{I}}\} = \mathbf{0}_{|\mathcal{I}|}$, and let other elements in $\mathbf{d}_{dl}$ to be 0, which means $[\mathbf{d}_{dl}]_{\{0,1,...D'-1\}-\mathcal{I}} = \mathbf{0}_{D'-|\mathcal{I}|}$. Notice that $[\mathbf{x}'_{dl}]_r$ is the rth element of the lth transmitted block $\mathbf{x}'_{dl}$, and $n = lD' + r$. The average autocorrelation function $R_{xd}[i]$ of $x_d[n]$, can be expressed as

$$R_{xd}[i] = \frac{1}{D'}\sum_{n=0}^{D'-1}\mathrm{E}\{x_d[n]x_d^*[n-i]\}$$

$$= \frac{1}{D'}\sum_{n=0}^{D'-1}\mathrm{E}\{[\mathbf{A}'\mathbf{d}_{dl}]_p[\mathbf{A}'\mathbf{d}_{dl'}]_{p'}^*\},$$

where $l' = \lfloor\frac{n-i}{D'}\rfloor$, $p' = \langle n-i\rangle_{D'}$, and $n - i = l'D' + p'$, and

$$R_{xd}[i] = \frac{1}{D'}\sum_{n=0}^{D'-1}\mathrm{E}\{[\mathbf{A}']_{p,:}\mathbf{d}_{dl'}([\mathbf{A}']_{p',:}\mathbf{d}_{dl'})^H\}.$$

It can be derived that $[\mathbf{A}']_{p,:}\mathbf{d}_{dl'} = \sum_{s=0}^{D-1}[\mathbf{A}']_{p,s}[\mathbf{d}_{dl'}]_s = \sum_{s\in\mathcal{I}}[\mathbf{A}']_{p,s}[\mathbf{d}_{dl'}]_s = [\mathbf{A}']_{p,\mathcal{I}}[\mathbf{d}_{dl'}]_{\mathcal{I}}$, then

$$= \frac{1}{D'}\sum_{n=0}^{D'-1}\mathrm{E}\{[\mathbf{A}']_{p,\mathcal{I}}[\mathbf{d}_{dl'}]_{\mathcal{I}}([\mathbf{A}']_{p',\mathcal{I}}[\mathbf{d}_{dl'}]_{\mathcal{I}})^H\}$$

$$= \frac{1}{D'}\sum_{n=0}^{D'-1}\mathrm{E}\{[\mathbf{A}']_{p',\mathcal{I}}[\mathbf{d}_{dl}]_{\mathcal{I}}[\mathbf{d}_{dl'}]_{\mathcal{I}}{}^H[\mathbf{A}']_{p',\mathcal{I}}{}^H\}$$

$$= \frac{1}{D'}\sum_{n=0}^{D'-1}[\mathbf{A}']_{p,\mathcal{I}}\,\mathrm{E}\{[\mathbf{d}_{dl}]_{\mathcal{I}}[\mathbf{d}_{dl'}]_{\mathcal{I}}{}^H\}[\mathbf{A}']_{p',\mathcal{I}}{}^H$$

$$= \frac{1}{D'}\sum_{n=0}^{D'-1}[\mathbf{A}']_{p,\mathcal{I}}\,\mathrm{E}\{[\mathbf{d}_{dl}]_{\mathcal{I}}[\mathbf{d}_{dl'}]_{\mathcal{I}}{}^H\}[\mathbf{A}']_{p',\mathcal{I}}{}^H,$$

and the autocorrelation matrix

$$\mathrm{E}\{[\mathbf{d}_{dl}]_{\mathcal{I}}[\mathbf{d}_{dl'}]_{\mathcal{I}}{}^H\} = \begin{cases} E_s\mathbf{I}_{|\mathcal{I}|}, & l = l' \\ 0, & \text{otherwise} \end{cases}.$$

When the conditions $l = l'$ and $n = 0, 1, 2...D' - 1$ are satisfied, that is $l = \lfloor\frac{n}{D'}\rfloor =$

doi:10.6342/NTU201902242

$\lfloor \frac{n-i}{D'} \rfloor = l'$, that implies $n-i = 0, 1, 2...D'-1$, $i = -(D'-1)...0, 1, 2...D'-1$, we could get $p = \langle n \rangle_{D'} = n$, and $p' = \langle n-i \rangle_{D'} = n-i$. We obtain

$$R_{xd}[i] = \frac{E_s}{D'} \sum_{n=0}^{D'-1} [\mathbf{A}']_{p,\mathcal{I}} [\mathbf{A}']_{p',\mathcal{I}}{}^H = \frac{E_s}{D'} \sum_{n=0}^{D'-1} [\mathbf{A}']_{n,\mathcal{I}} [\mathbf{A}']_{n-i,\mathcal{I}}{}^H$$

$$= \frac{E_s}{D'} \sum_{n=0}^{D'-1} \sum_{s\in\mathcal{I}} [\mathbf{A}']_{n,s} [\mathbf{A}'^H]_{s,n-i} = \frac{E_s}{D'} \sum_{n=0}^{D'-1} \sum_{s\in\mathcal{I}} [\mathbf{A}']_{n,s} [\mathbf{A}']^*_{n-i,s}.$$

We define

$$a_s[m] = \begin{cases} [\mathbf{A}']_{m,s}, & m = 0, 1, ..., D'-1 \\ 0, & \text{otherwise,} \end{cases} \tag{A.23}$$

, and denote the DTFT operation as in

$$A_s(e^{j\omega}) = \text{DTFT}_m\ (a_s[m]) = \sum_{m=0}^{D'-1} [\mathbf{A}']_{m,s} e^{-j\omega m}.$$

We write the autocorrelation function as

$$R_x[i] = \frac{E_s}{D'} \sum_{n=0}^{D'-1} \sum_{s\in\mathcal{I}} [\mathbf{A}']_{n,s} [\mathbf{A}']^*_{n-i,s} = \frac{E_s}{D'} \sum_{n=0}^{D'-1} \sum_{s\in\mathcal{I}} [\mathbf{A}']_{n,s} a_s[n-i]^* \tag{A.24}$$

and get the PSD by using the DTFT with time reversal, time conjugation, time shifting, and frequency shifting properties,

$$S_x(e^{j\omega}) = \text{DTFT}_i\ (R_x[i]) = \frac{E_s}{D'} \sum_{n=0}^{D'-1} \sum_{s\in\mathcal{I}} [\mathbf{A}']_{n,s} \text{DTFT}_i\ (a_s[n-i]^*)$$

$$= \frac{E_s}{D'} \sum_{n=0}^{D'-1} \sum_{s\in\mathcal{I}} [\mathbf{A}']_{n,s} A_s(e^{j\omega})^* e^{-j\omega n}$$

$$= \frac{E_s}{D'} \sum_{s\in\mathcal{I}} A_s(e^{j\omega})^* \sum_{n=0}^{D'-1} [\mathbf{A}']_{n,s} e^{-j\omega n}$$

$$= \frac{E_s}{D'} \sum_{s\in\mathcal{I}} A_s(e^{j\omega})^* A_s(e^{j\omega})$$

doi:10.6342/NTU201902242

$$= \frac{E_s}{D'} \sum_{s \in \mathcal{I}} |A_s(e^{j\omega})|^2 = \frac{E_s}{D'} \sum_{s \in \mathcal{I}} | \sum_{m=0}^{D'-1} [\mathbf{A'}]_{m,s} e^{-j\omega m}|^2 = \frac{E_s}{D'} \| (\mathbf{v}_{D'}(e^{j\omega})^H [\mathbf{A'}]_{:,\mathcal{I}})^T \|^2 . \tag{A.25}$$

Substituting (A.25) into (A.1), we finally get the power spectrum of $x_a(t)$

$$S_a(f) = \frac{E_s |P(f)|^2}{D' T_s} \sum_{s \in \mathcal{I}} |A_s(e^{j2\pi f T_s})|^2 = \frac{E_s |P(f)|^2}{D' T_s} \| (\mathbf{v}_{D'}(e^{j2\pi f Ts})^H [\mathbf{A'}]_{:,\mathcal{I}})^T \|^2 . \tag{A.26}$$

□

doi:10.6342/NTU201902242